
NEUROCHAOS FEATURE TRANSFORMATION AND CLASSIFICATION FOR IMBALANCED LEARNING

Deeksha Sethi

Department of Electronics and Communication Engineering
BMS Institute of Technology and Management
Bengaluru - 560064, Karnataka, India
deeksha.sethi03@gmail.com

Nithin Nagaraj

Consciousness Studies Programme
National Institute of Advanced Studies
Indian Institute of Science Campus
Bengaluru - 560012, Karnataka, India
nithin@nias.res.in

Harikrishnan N B

Consciousness Studies Programme
National Institute of Advanced Studies
Indian Institute of Science Campus
Bengaluru - 560012, Karnataka, India

The University of Trans-Disciplinary Health Sciences And Technology
Bengaluru - 560064, Karnataka, India
harikrishnannb07@gmail.com

May 17, 2022

ABSTRACT

Learning from limited and imbalanced data is a challenging problem in the Artificial Intelligence community. Real-time scenarios demand decision-making from rare events wherein the data are typically imbalanced. These situations commonly arise in medical applications, cybersecurity, catastrophic predictions etc. This motivates development of learning algorithms capable of learning from imbalanced data. Human brain effortlessly learns from imbalanced data. Inspired by the chaotic neuronal firing in the human brain, a novel learning algorithm namely *Neurochaos Learning* (NL) was recently proposed. NL is categorized in three blocks: Feature Transformation, Neurochaos Feature Extraction (CFX), and Classification. In this work, the efficacy of neurochaos feature transformation and extraction for classification in imbalanced learning is studied. We propose a unique combination of neurochaos based feature transformation and extraction with traditional ML algorithms. The explored datasets in this study revolve around medical diagnosis, banknote fraud detection, environmental applications and spoken-digit classification. In this study, experiments are performed in both high and low training sample regime. In the former, five out of nine datasets have shown a performance boost in terms of macro F1-score after using CFX features. The highest performance boost obtained is **25.97%** for *Statlog (Heart)* dataset using CFX+Decision Tree. In the low training sample regime (from just one to nine training samples per class), the highest performance boost of **144.38%** is obtained for *Haberman's Survival* dataset using CFX+Random Forest. NL offers enormous flexibility of combining CFX with any ML classifier to boost its performance, especially for learning tasks with limited and imbalanced data.

1 Introduction

Technological advancements have made a paradigm shift in the evolution of science. A driving force behind this shift is the high storage and computational capacity available in this era. This has given rise to computational techniques for analysis and pattern discovery from data, popularly known as *data-driven science*. Data can be structured or

unstructured. In today’s world the data analytics techniques have to make sense from big data. This demands intelligent approaches towards meaningful feature extraction from data and thereby contribute to decision making. The bedrock for this approach of data-driven science comes under the purview of Artificial Intelligence (AI). Artificial Intelligence (AI) can be defined as an anarchy of methods [1]. This anarchy involves (a) Symbolic AI (logic-based AI), (b) Statistical Learning (Machine Learning), and (c) Sub-Symbolic AI (brain-inspired learning) [2]. The aforementioned verticals of AI have seen a remarkable progress in recent past. On the other hand, these approaches are limited when it comes to decision making under the presence of rare events [3].

Rare events by definition are events whose frequency of occurrence are significantly less compared to more frequently occurring events [4]. Some examples of rare events are: outbreak of a pandemic [5, 6], cyber attack [7], fraudulent transactions [8] and natural disasters [4]. In this scenario, it is critical to provide an early warning response to take appropriate decisions. Hence, the accurate prediction or classification of rare events is of immense importance. Failing to do so can lead to a catastrophe. For example, in the case of COVID-19 pandemic, wrongly classifying a positive person can increase the spread rate of the viral infection. To curb the spread, it is important to correctly classify the infected people and take appropriate measures. Thus, the major challenge in the classification of all rare events is the lack of sufficient data. This boils down to the problem of imbalanced learning. Imbalanced learning deals with an unequal distribution of data instances amongst distinct classes of a dataset. This can mean either one or more classes in a dataset have relatively greater number of data instances as compared to the remaining classes [3]. Frequently implemented approaches to imbalanced learning can be categorized into (a) pre-processing strategies [3] and (b) cost sensitive learning [9]. The main idea behind pre-processing methods is to optimize the feature space and thereby perform classification by ensemble or algorithmic techniques [3]. On the other hand, cost-sensitive learning assigns a cost (penalty) for every misclassification, with the end goal of minimizing the overall cost [9].

One widely used pre-processing technique is resampling. Resampling restores balance in the sample space by modifying the samples as follows:

1. Over-sampling: This approach addresses resampling by generating new samples for the minority classes. Ex: SMOTE [10].
2. Under-sampling: This type of resampling is done by eliminating the innate samples in the majority classes. Ex: Random Under-Sampling [11].

Combinations of over-sampling and under-sampling methods are known as hybrid methods.

Another common pre-processing technique involves feature selection and feature extraction. Feature selection provides a subset of original input features. Whereas, feature extraction does a functional mapping of input features to generate new features [3]. Principal Component Analysis [12], Dynamic Mode Decomposition [13], Mel-scale Frequency Cepstral Coefficient [14], Non Negative Matrix Factorization [15], Empirical Mode Decomposition [16] etc. are examples of feature extraction algorithms. A detailed study on pre-processing, feature selection and feature extraction are provided in [3]. It should be noted that most of these methods make use of *linear* transformations.

In this paper, we explore a recent study on a nonlinear chaos based learning algorithm namely *Neurochaos Learning* (NL), proposed in [17, 18]. NL draws its inspiration from the *nonlinear chaotic firing* that is intrinsic to neurons in the brain. The human brain is a highly complex system with an estimated 86 billion interconnected neurons [19]. Individual neurons in the human brain are known to exhibit a wide variety of behaviors – ranging from periodic, quasi-periodic to fully chaotic. Chaos is central to the brain since chaotic behaviour is found at different spatiotemporal scales starting from individual neurons to networks of neurons [20].

NL also addresses an essential practice in Machine Learning: Feature transformation. NL proposes a novel approach by transforming pre-existing features into chaos-based features [17]. These features are passed to a classifier for decision making. For the first time, in [17], the authors employ the rich properties of chaos in learning algorithms for classification. Also, a performance boost in classification in the few-shot learning regime has been shown using chaos-based-features in [17, 21].

The effectiveness of NL is shown in the classification of various datasets such as *MNIST*, *Iris*, *Exoplanet* [17], *Coronavirus Genome classification* [21], especially in the low training sample regime. Recently, [22] has demonstrated the efficacy of NL in the classification and preservation of cause-effect for 1D coupled chaotic maps and coupled AR processes.

There is a need to rigorously test NL, and in particular the nonlinear chaotic transformation of features, to more datasets in the context of imbalanced learning. This study addresses this gap. We combine NL features with classical machine learning algorithms such as Decision Tree (DT), Random Forest (RF), AdaBoost (AB), Support Vector Machine (SVM), *k*-Nearest Neighbors (*k*-NN) and Gaussian Naive Bayes (GNB). A comparison of NL: chaos-based-hybrid ML architectures with stand-alone ML algorithms is brought out for the following balanced and imbalanced datasets: *Iris*,

Ionosphere, Wine, Bank Note Authentication, Haberman's Survival, Breast Cancer Wisconsin, Statlog (Heart), Seeds, Free Spoken Digit Dataset. A detailed analysis of this comparative study (NL: chaos-based-hybrid ML vs. stand-alone ML) is carried out for both the high and low training sample regime. Learning from limited data/ imbalanced data is a challenging problem in the ML community. This research highlights the performance comparison of NL and classical ML algorithms in learning from limited training instances.

The organization of this paper is as follows: section 2 explains the proposed architecture and methods being investigated in this paper. The description of all datasets used for the experiments is provided in section 3. The experiments and their corresponding results are available in section 4. A detailed discussion on the inferences is provided in section 5. The concluding remarks of this study are in section 6.

2 Proposed Method

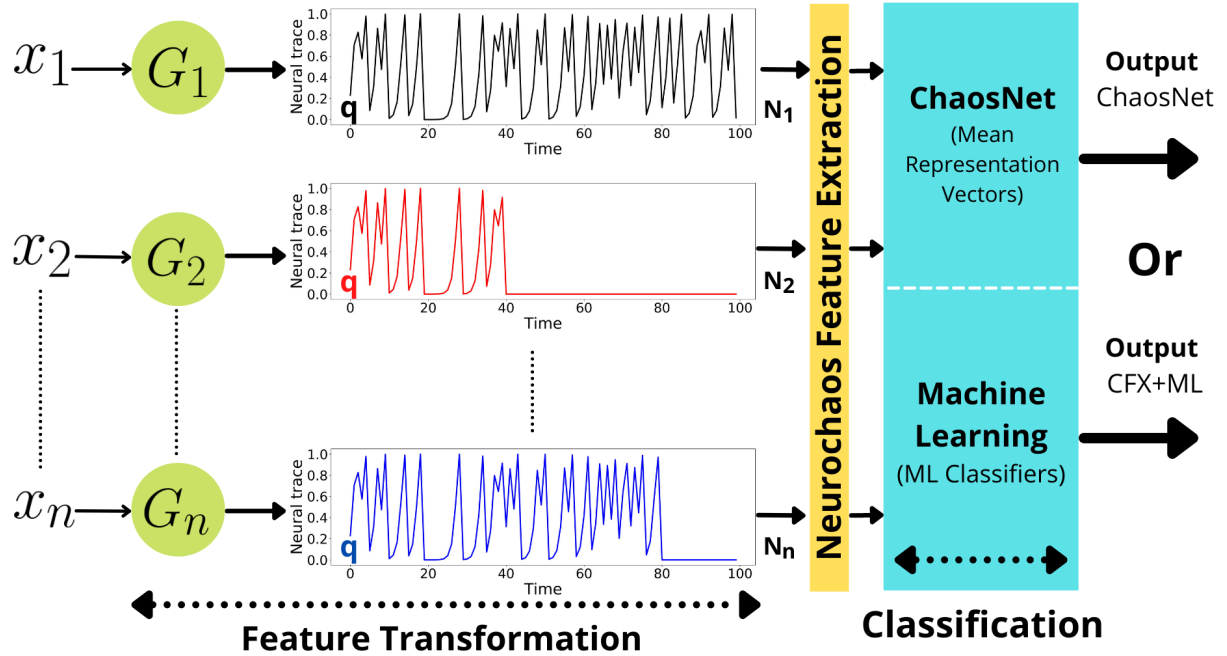


Figure 1: The three steps proposed in this study. (a) feature transformation, (b) neurochaos feature extraction, and (c) classification. The classifier chosen could either be ChaosNet or any other ML classifier.

In this study, a modified form of the recently proposed Neurochaos Learning architecture [18] is put forward. This modified NL architecture is depicted in Figure 1. NL has mainly three blocks - (a) feature transformation, (b) neurochaos feature extraction and (b) classification. A detailed description of each block is given below.

- **Input:** Input is the first and most significant step of any learning process. It contains input attributes obtained from the dataset (x_1, x_2, \dots, x_n) . These input attributes (after suitable normalization) are further passed to the feature transformation block.
- **Feature Transformation:** The feature transformation block consists of an input layer of 1D Generalized Lüroth Series (GLS) neurons. The 1D GLS neurons are piece-wise linear chaotic maps. The number of GLS neurons (G_1, G_2, \dots, G_n) in the input layer is equal to the number of input attributes (n) in the dataset. Each neuron G_1, G_2, \dots, G_n has an initial neural activity of q units. Upon arrival of the input attributes (also known as *stimuli*) x_1, x_2, \dots, x_n , each of the 1D GLS neurons (G_1, G_2, \dots, G_n) starts independently firing with an initial neural activity of q units. The neural trace of these chaotic neurons halts when it reaches the ϵ neighbourhood of the stimulus (at which point we say that it has successfully recognized the stimulus). The halting of the neural trace is mathematically guaranteed by the topological transitivity property of chaos [17]. The transformed input attributes are further passed to the neurochaos feature extraction block.
- **Neurochaos Feature Extraction:** The following features are extracted from the chaotic neural trace:

1. *Firing time* (N): The time taken by the chaotic neural trace to recognise the stimulus [23].
2. *Firing rate* (R): Fraction of time for which the chaotic neural trace exceeds the discrimination threshold b so as to recognize the stimulus [23].
3. *Energy* (E): A chaotic neural trace $z(t)$ with a firing time N has an energy (E) defined as:

$$E = \sum_{t=1}^N z(t)^2. \quad (1)$$

4. *Entropy* (H): The entropy of a chaotic neural trace $z(t)$ is computed using the symbolic sequence $SS(t)$ of $z(t)$. $SS(t)$ is defined as follows:

$$SS(t_i) = \begin{cases} 0, & z(t_i) < b, \\ 1, & b \leq z(t_i) < 1, \end{cases} \quad (2)$$

where $i = 1$ to N (firing time). From $SS(t)$, Shannon Entropy $H(SS)$ is computed as follows:

$$H(SS) = - \sum_{i=1}^2 p_i \log_2(p_i) \text{ bits}, \quad (3)$$

where, p_1 and p_2 are the probabilities of occurrence of symbols 0 and 1 in $SS(t)$ respectively.

An input stimulus x_k of a data instance visiting the k -th GLS neuron (G_k) is transformed to a 4D vector $[N_{x_k}, R_{x_k}, E_{x_k}, H_{x_k}]$. The CFX feature space contains a collection of all the 4D vectors after feature transformation. These chaos based features are passed to the third block of the NL architecture i.e., classification.

- **Classification:** There are mainly two kinds of NL architecture: (a) ChaosNet, (b) ChaosFEX (CFX) + ML. ChaosNet architecture computes the mean representation vector for each class. The mean representation vector of class- k contains the mean firing time, mean firing rate, mean energy and mean entropy of the k -th class. ChaosNet uses a simplistic decision rule, namely, the cosine similarity of testdata instances with the mean representation vectors. The testdata instance is assigned a label $= l$, if the cosine similarity of that testdata instance with l -th mean representation vector is the highest.

Alternatively, we have the flexibility of choosing any other ML classifier instead of ChaosNet. In this kind of NL architecture, the ChaosFEX features are fed directly to the ML classifier (CFX+ML). In this study, we have tested with the following ML algorithms – Decision Tree (DT), Random Forest (RF), AdaBoost (AB), Support Vector Machine (SVM), k -Nearest Neighbors (k -NN) and Gaussian Naive Bayes (GNB). CFX+ML is a hybrid NL architecture that combines the best of chaos and machine learning.

- **Output:** The output obtained from the classification block serves as output for that respective NL architecture. On using ChaosNet in the classification block, the output is an outcome of classification based on the mean representation vectors. The Machine Learning implementation in the classification block produces an output dependent on the choice of the ML classifier.

In [21], it has been shown that ChaosNet satisfies the *Universal Approximation Theorem* with a bound on the number of chaotic neurons to approximate the finite support discrete time function. This is due to the uncountably infinite number of dense orbits and the *topological transitivity* property of chaos. Another important feature of ChaosNet and CFX+ML is the natural presence of Stochastic Resonance (noise enhanced signal processing) [18] found in the architecture. An optimal performance of ChaosNet and CFX+ML is obtained for an intermediate value of noise intensity (ϵ). This has been thoroughly shown in [18].

3 Dataset Description

The ChaosFEX (CFX) feature extraction algorithm requires normalization of the dataset and numeric codes for labels. Therefore, to maintain uniformity, all datasets are normalized¹ for both stand-alone algorithms and their integration with CFX. The labels are renamed to begin from zero in each dataset to ensure compatibility with CFX feature extraction. The rules followed for the numeric coding for the labels of all the datasets are provided in section 8 (Table 16 - 24).

¹ $X_{norm} = \frac{X - \min(X)}{\max(X) - \min(X)}.$

3.1 Iris

Iris [24, 25] aids classification of three iris plant variants: Iris Setosa, Iris Versicolour, and Iris Virginica. There are 150 data instances in this dataset with four attributes in each data instance: sepal length, sepal width, petal length, and petal width. All attributes are in *cms*. The specified class distribution provided in Table 1 is in the following order: (Setosa, Versicolour, Virginica).

3.2 Ionosphere

The *Ionosphere* [26, 27] dataset enables a binary classification problem. The classes represent the status of returning a radar signal from the Ionosphere. Label ‘g’ (Good) denotes the return of the radar signal, and label ‘b’ (Bad) indicates no trace of return of the radar signal. The goal of this experiment is to identify the structure of the Ionosphere using radar signals. This dataset has 351 data instances and 34 attributes. The specified class distribution provided in Table 1 is as follows: (Bad, Good).

3.3 Wine

Wine [26, 28] dataset aims to identify the origin of different wines using chemical analysis. The classes are labeled ‘1’, ‘2’, and ‘3’. It has 178 data instances and 13 attributes ranging from alcohol, malic acid to hue and proline for the collected samples. The specified class distribution provided in Table 1 is as follows: (1, 2, 3).

3.4 Bank Note Authentication

Bank-note Authentication [26, 29] is a binary classification dataset. The classes involve Genuine and Forgery. A Genuine class refers to an authentic banknote denoted by ‘0’, while a Forgery class refers to a forged banknote denoted by ‘1’. The obtained dataset is from images of banknotes belonging to both classes, taken from an industrial camera. It contains 1372 total data instances. The dataset has four attributes retrieved from the images using wavelet transformation. The specified class distribution provided in Table 1 is as follows: (Genuine, Forgery).

3.5 Haberman’s Survival

Haberman’s Survival [26, 30] is a compilation of sections of a study investigating the lifespan of a patient after undergoing a breast cancer surgery. This is a binary classification problem and the dataset provides information for the prediction of the survival of patients beyond five years. Class ‘1’ denotes survival of the patient for five years or longer after the surgery. Class ‘2’ denotes the death of a patient within five years of the surgery. It contains 306 total data instances and three attributes. The specified class distribution provided in Table 1 is as follows: (1, 2).

3.6 Breast Cancer Wisconsin

Breast Cancer Wisconsin [26, 31] dataset deals with the classification of the intensity of the breast cancer. Class ‘M’ refers to a malignant level of infection and class ‘B’ refers to a benign level of infection. It contains a total of 569 data instances and 31 attributes such as radius, perimeter, texture, smoothness, etc. for each cell nucleus. The specified class distribution provided in Table 1 is as follows: (Malignant - M, Benign - B).

3.7 Statlog (Heart)

Statlog (Heart) [26] enables differentiation between presence and absence of a heart disease in a patient. Class ‘1’ denotes the absence while class ‘2’ denotes the presence of a heart disease. It contains 270 total data instances and 13 attributes including resting blood pressure, chest pain type, exercise induced angina and so on. The specified class distribution provided in Table 1 is as follows: (Absence, Presence).

3.8 Seeds

Seeds [26] dataset examines three classes of wheat: Kama, Rosa and Canadian using soft X-ray on the wheat kernels to retrieve relevant properties. It contains 210 total data instances and seven attributes namely compactness, length, width etc. of each wheat kernel. The specified class distribution provided in Table 1 is as follows: (Kama, Rosa, Canadian).

3.9 Free Spoken Digit Dataset

The *Free Spoken Digit Dataset* [32] is a time-series dataset comprising recordings of six speakers. Each speaker recites numbers from one to nine. For each number, every speaker makes 50 recordings. The speaker chosen for all experiments is Jackson. The dataset undergoes preprocessing using a Fast Fourier Transform (FFT) technique. The dataset for speaker Jackson has 500 data instances, and only instances above a threshold of 3000 samples are considered to tackle the varying data length through the dataset. In these data instances, only the first 3005 data samples are examined. Finally, 480 data instances are filtered to feed into the algorithm. The specified class distribution provided in Table 1 is as follows: (0, 1, 2, 3, 4, 5, 6, 7, 8, 9).

Table 1: Train-Test split in experiments. High training sample regime corresponds to an 80% and 20% split in training and testing respectively. In the Imbalanced data column, ‘Y’ implies yes and ‘N’ implies no.

Dataset	Classes	Features	Training samples /class	Testing samples /class	Imbalanced data (Y/N)
Iris	3	4	(40, 41, 39)	(10, 9, 11)	N
Ionosphere	2	34	(98, 182)	(28, 43)	Y
Wine	3	13	(45, 57, 40)	(14, 14, 8)	Y
Bank Note Authentication	2	4	(614, 483)	(148, 127)	Y
Haberman’s Survival	2	3	(181, 63)	(44, 18)	Y
Breast Cancer Wisconsin	2	31	(169, 286)	(43, 71)	Y
Statlog (Heart)	2	13	(117, 99)	(33, 21)	Y
Seeds	3	7	(59, 56, 53)	(11, 14, 17)	N
FSDD	10	3005	(40, 35, 44, 42, 38, 34, 37, 44, 33, 37)	(10, 15, 6, 8, 8, 7, 13, 6, 10, 13)	Y

4 Experiments & Results

In this section, the authors evaluate the efficacy of ChaosFEX (CFX) feature engineering on various classification tasks. For this, hybrid models are developed by combining CFX features extracted from the input data with the classical ML algorithms such as Decision Tree, Random Forest, AdaBoost, Support Vector Machine, k -Nearest Neighbors and Gaussian Naive Bayes. The experiments are performed for both low and high training sample regime. The train-test distribution (80% – 20%) for each dataset in the high training sample regime is available in Table 1. In low training sample regime, 150 random trials for training with 1, 2, \dots , 9 data instances per class are considered. The trends of all algorithms in the stand-alone form and their implementation using CFX features are conveyed in this section. For all experiments in the paper, the following software: Python 3.8 and scikit-learn [24], CFX [17] are used.

4.1 Hyperparameter Tuning

Every ML algorithm has a set of optimal hyperparameters to be found by hyperparameter tuning. The hyperparameters for all the algorithms with respect to each dataset were tuned using five-fold cross-validation. Table 2 provides the set of hyperparameters tuned for all algorithms in this research.

In the case of CFX+ML for *Iris*, *Ionosphere* and *Wine*, both CFX (q, b, ϵ) and ML hyperparameters were tuned. For the remaining datasets, the hyperparameters tuned for ChaosNet (q, b, ϵ) were retained and only the ML hyperparameters were tuned.

4.2 Performance Metric

The most common performance metric used in ML is *Accuracy* [33]. In the case of imbalanced datasets, this metric will lead to misinterpretation of results. Thus, the performance metric used for all experiments in this study is *Macro F1-Score*. This metric is computed from the confusion matrix. Figure 2 shows a confusion matrix for a binary classification problem. Prediction values represent the predictions made by the classifier. Actual values stand for the

Table 2: References for the tuned hyperparameters for all algorithms. Owing to space constraints, most of the tables are moved to the Supplementary Information section (section 8).

Algorithm	Acronyms	Hyperparameters Tuned	Reference
ChaosNet	-	q, b, ϵ	Tables 4, 5, 6, 7, 8, 9, 10, 11 and 12
Decision Tree	DT	$min_samples_leaf,$ $max_depth,$ ccp_alpha	Tables 25 and 26 in Supplementary Information section
Random Forest	RF	$n_estimators,$ max_depth	Tables 27 and 28 in Supplementary Information section
AdaBoost	AB	$n_estimators$	Table 29 in Supplementary Information section
Support Vector Machine	SVM	$C, kernel$	Table 30 in Supplementary Information section
k -Nearest Neighbors	k -NN, KNN	k	Table 31 in Supplementary Information section
Gaussian Naive Bayes	GNB	-	-

true/ target values for the predictions being made by the classifier. They both have two categories: Positive and Negative. A true positive stands for a target value equal to positive, also correctly classified by the classifier as positive. True negatives are target values equal to negative, also correctly classified by the classifier as negative. False negative implies a target value equal to positive which was incorrectly classified as negative by the classifier. Similarly, false positive means a target value equal to negative that was incorrectly classified as positive by the classifier.

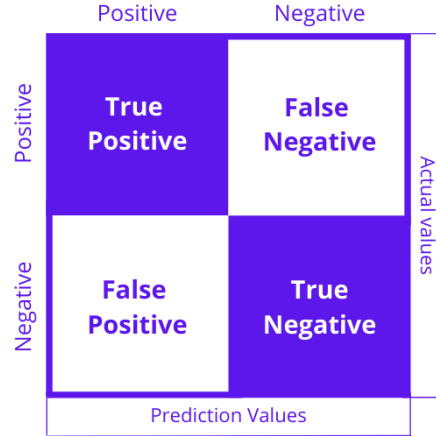


Figure 2: Pictorial representation of a confusion matrix corresponding to a binary classification problem.

F1-Score depends on two parameters:

1. Precision - The ratio of the number positives correctly classified as positive by the algorithm to the total number of instances classified as positive, given by -

$$Precision = \frac{True\ Positive}{True\ Positive + False\ Positive}. \quad (4)$$

2. Recall - The ratio of the number positives correctly classified as positive by the algorithm to the total number of actual positives, given by -

$$Recall = \frac{True\ Positive}{True\ Positive + False\ Negative}. \quad (5)$$

Thus, F1-Score which is the harmonic mean of Precision and Recall is given by,

$$F1-Score(F1) = \frac{2 \cdot Precision \cdot Recall}{Precision + Recall}. \quad (6)$$

Macro F1-Score is obtained by averaging the F1 scores for all classes in the dataset, given by

$$Macro\ F1-Score = \frac{F1_{Class-1} + F1_{Class-2} + \dots + F1_{Class-n}}{n}, \quad (7)$$

where, n stands for the number of distinct classes in the dataset. F1-score of $Class_k$ considers the instances of $Class_k$ as positive and all remaining instances of classes as negative. Thus, the task is transformed to a binary classification problem. All instances of $Class_k$ correctly classified as positive or negative by the classifier are termed as true positives or true negatives respectively. All instances that are incorrectly classified by the classifier are placed under the false positive and false negative category accordingly. Hence the associated equations of precision and recall for this example are given by,

$$Precision_{Class_k} (P_k) = \frac{True\ Positive_{Class_k}}{True\ Positive_{Class_k} + False\ Positive_{Class_k}}, \quad (8)$$

$$Recall_{Class_k} (R_k) = \frac{True\ Positive_{Class_k}}{True\ Positive_{Class_k} + False\ Negative_{Class_k}}. \quad (9)$$

The F1-score for $Class_k$ is computed by:

$$F1-Score_{Class_k} = \frac{2 \cdot P_k \cdot R_k}{P_k + R_k}. \quad (10)$$

Similarly, the F1-scores for all classes in the classification problem are computed and applied in Eq 7.

4.3 Performance of ChaosNet

ChaosNet has three hyperparameters – initial neural activity (q), discrimination threshold (b), and noise intensity (ϵ) [18]. Specifics of the same are provided in Table 2.

Table 3: ChaosNet results: High training sample regime results for the nine datasets used in the experiments.

Dataset	Macro-F1 Score (Test Data)
Iris	1.000
Ionosphere	0.860
Wine	0.976
Bank Note Authentication	0.845
Haberman's Survival	0.560
Breast Cancer Wisconsin	0.927
Statlog (Heart)	0.738
Seeds	0.845
FSDD	0.897

4.4 Comparative Performance Evaluation

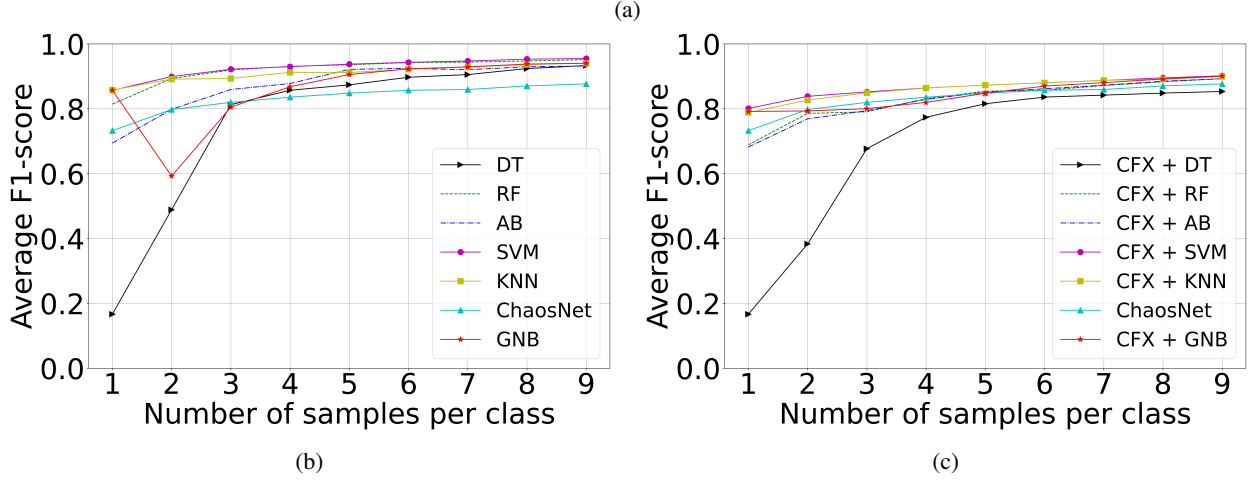
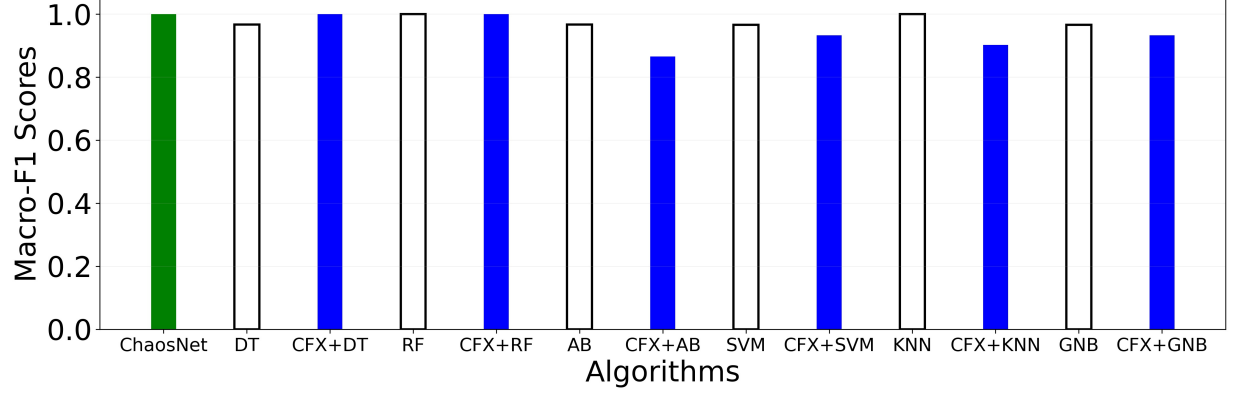
In this section, the authors represent the results in two formats (a) bar graph and (b) line graph. The comparative results for ChaosNet, CFX+ML and stand-alone ML in the high training sample regime are depicted using bar graph. All values plotted in the bar graphs for each dataset are provided in the Supplementary Information section (section 8) from Table 32 - 37. On the other hand, the line graph depicts the comparative performance of ChaosNet, CFX+ML and stand-alone ML in the low training sample regime.

4.4.1 Results for Iris

The tuned hyperparameters used and all experiment results for the *Iris* dataset are available in Table 4 and Figure 3 respectively.

Table 4: Hyperparameters used for *Iris* dataset for high and low training sample regime experiments.

Hyperparameter	Tuned Value
q	0.141
b	0.499
ϵ	0.147

Figure 3: *Iris*. (a) High training sample regime. (b) Comparative performance of stand-alone algorithms in the low training sample regime. (c) Comparative performance of CFX+ML algorithms in the low training sample regime.

4.4.2 Results for Ionosphere

The tuned hyperparameters used and all experiment results for the *Ionosphere* dataset are available in Table 5 and Figure 4 respectively.

Table 5: Hyperparameters used for *Ionosphere* dataset for high and low training sample regime experiments.

Hyperparameter	Tuned Value
q	0.680
b	0.969
ϵ	0.164

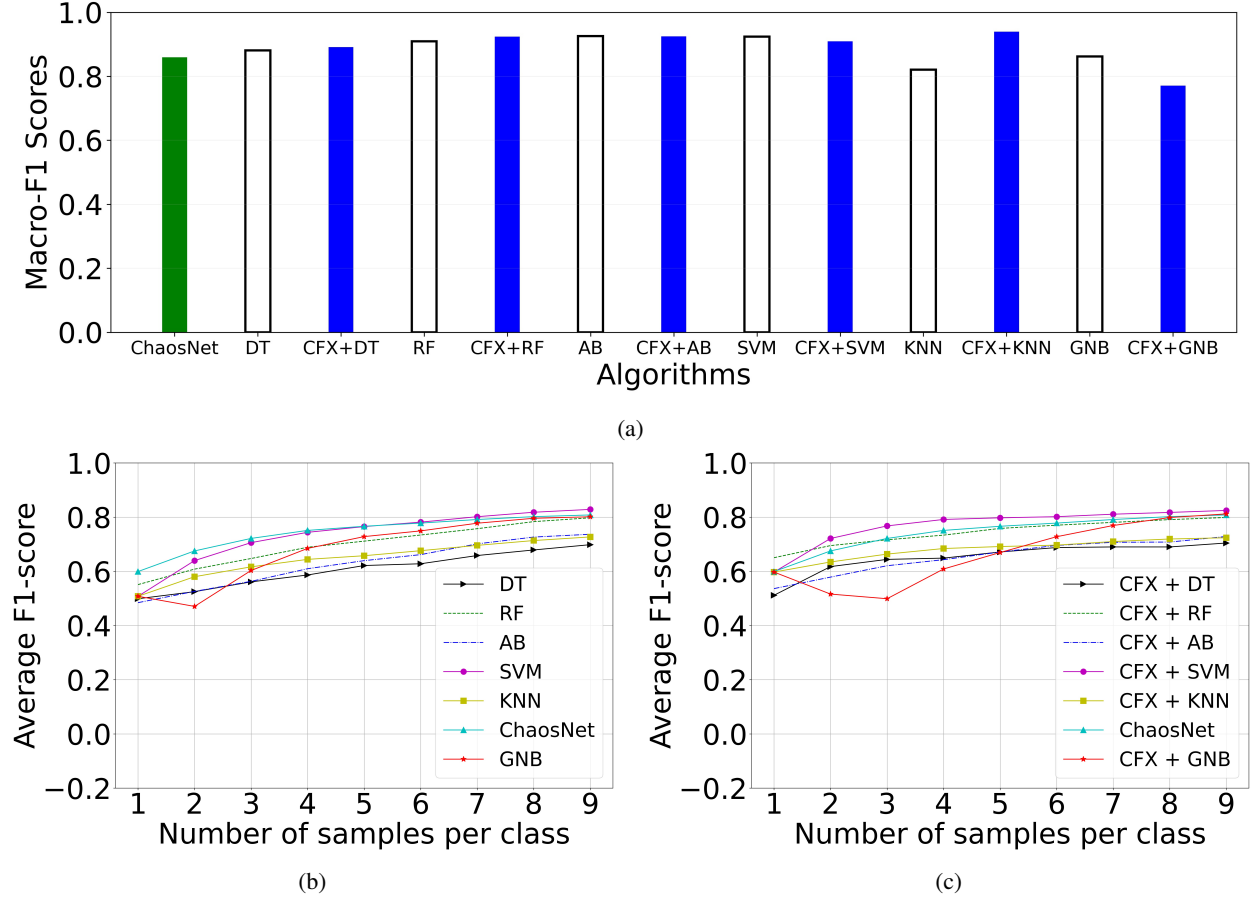


Figure 4: *Ionosphere*. (a) High training sample regime. (b) Comparative performance of stand-alone algorithms in the low training sample regime. (c) Comparative performance of CFX+ML algorithms in the low training sample regime.

4.4.3 Results for Wine

The tuned hyperparameters used and all experiment results for the *Wine* dataset are available in Table 6 and Figure 5 respectively.

Table 6: Hyperparameters used for *Wine* dataset for high and low training sample regime experiments.

Hyperparameter	Tuned Value
q	0.790
b	0.499
ϵ	0.262

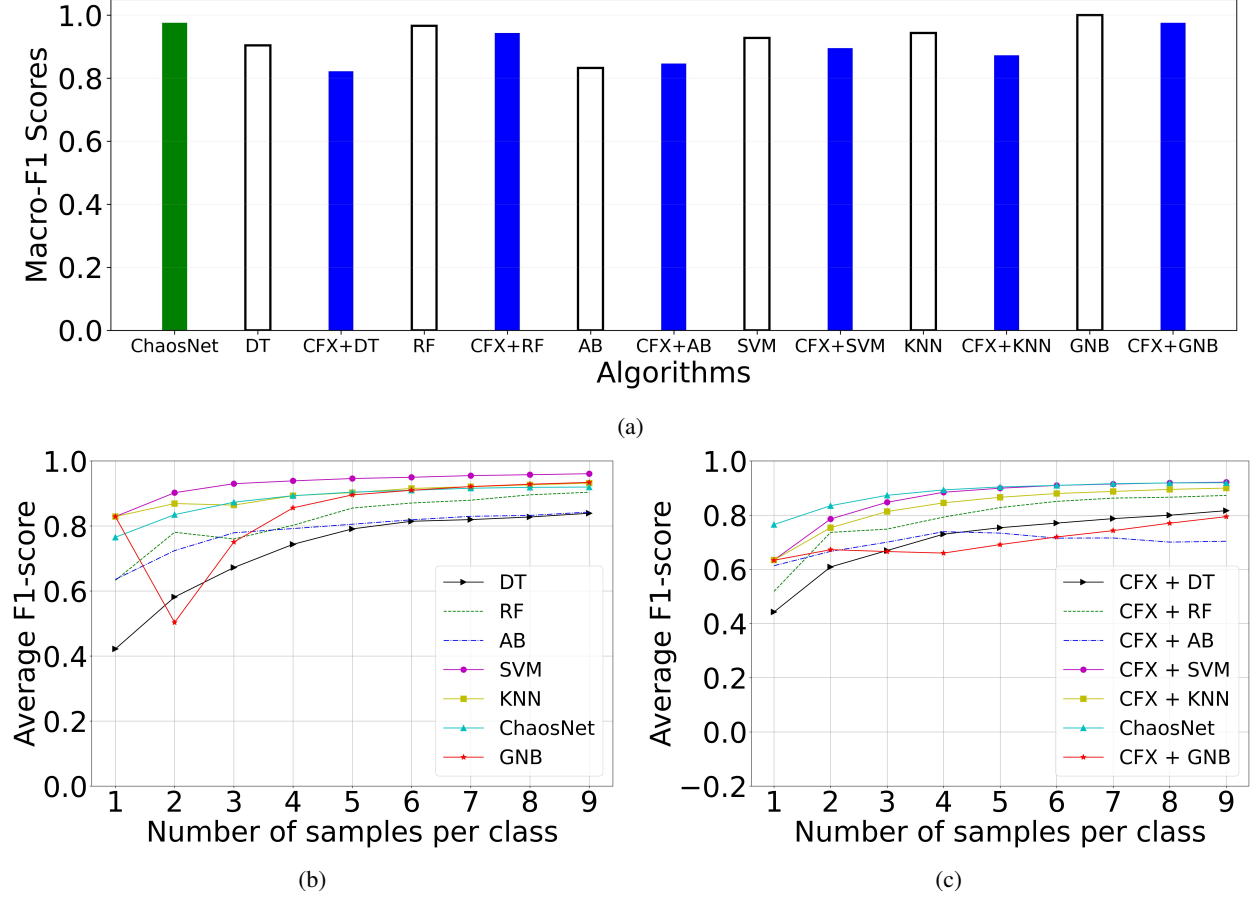


Figure 5: *Wine*. (a) High training sample regime. (b) Comparative performance of stand-alone algorithms in the low training sample regime. (c) Comparative performance of CFX+ML algorithms in the low training sample regime.

4.4.4 Results for Bank Note Authentication

The tuned hyperparameters used and all experiment results for the *Bank Note Authentication* dataset are available in Table 7 and Figure 6 respectively.

Table 7: Hyperparameters used for *Bank Note Authentication* dataset for high and low training sample regime experiments.

Hyperparameter	Tuned Value
q	0.080
b	0.250
ϵ	0.233

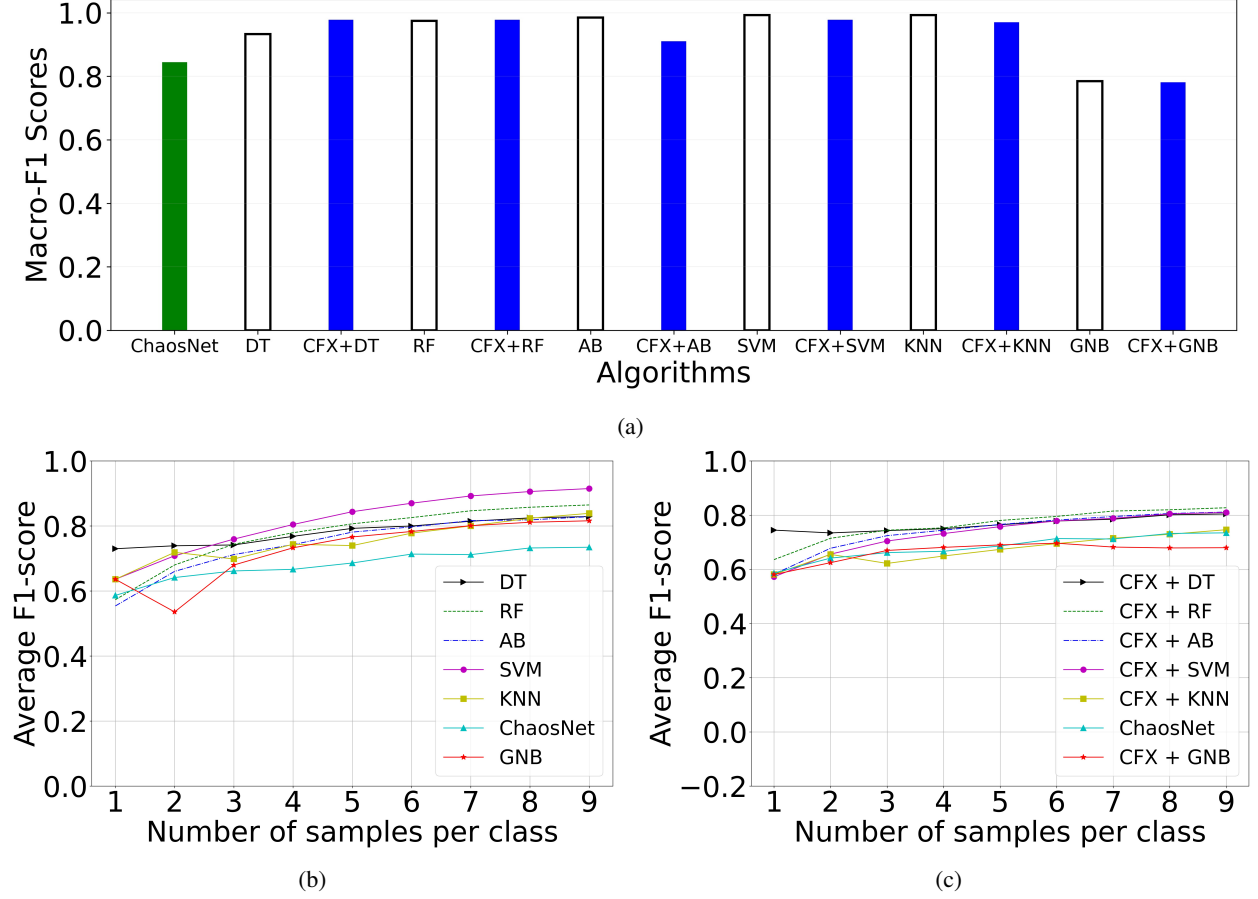


Figure 6: *Bank Note Authentication*. (a) High training sample regime. (b) Comparative performance of stand-alone algorithms in the low training sample regime. (c) Comparative performance of CFX+ML algorithms in the low training sample regime.

4.4.5 Results for Haberman's Survival

The tuned hyperparameters used and all experiment results for the *Haberman's Survival* dataset are available in Table 8 and Figure 7 respectively.

Table 8: Hyperparameters used for *Haberman's Survival* dataset for high and low training sample regime experiments.

Hyperparameter	Tuned Value
q	0.810
b	0.140
ϵ	0.003

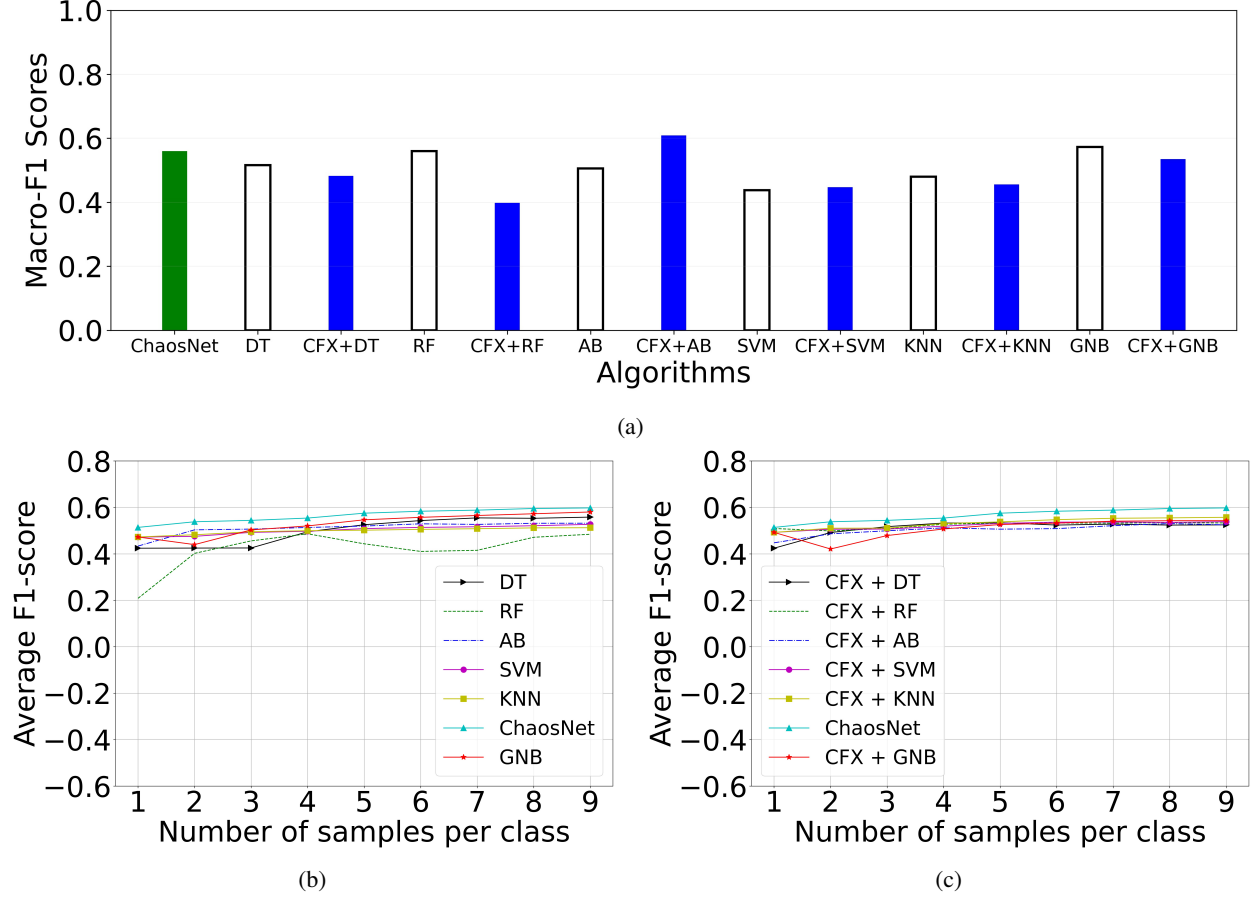


Figure 7: *Haberman's Survival*. (a) High training sample regime. (b) Comparative performance of stand-alone algorithms in the low training sample regime. (c) Comparative performance of CFX+ML algorithms in the low training sample regime.

4.4.6 Results for Breast Cancer Wisconsin

The tuned hyperparameters used and all experiment results for the *Breast Cancer Wisconsin* dataset are available in Table 9 and Figure 8 respectively.

Table 9: Hyperparameters used for *Breast Cancer Wisconsin* dataset for high and low training sample regime experiments.

Hyperparameter	Tuned Value
q	0.930
b	0.490
ϵ	0.159

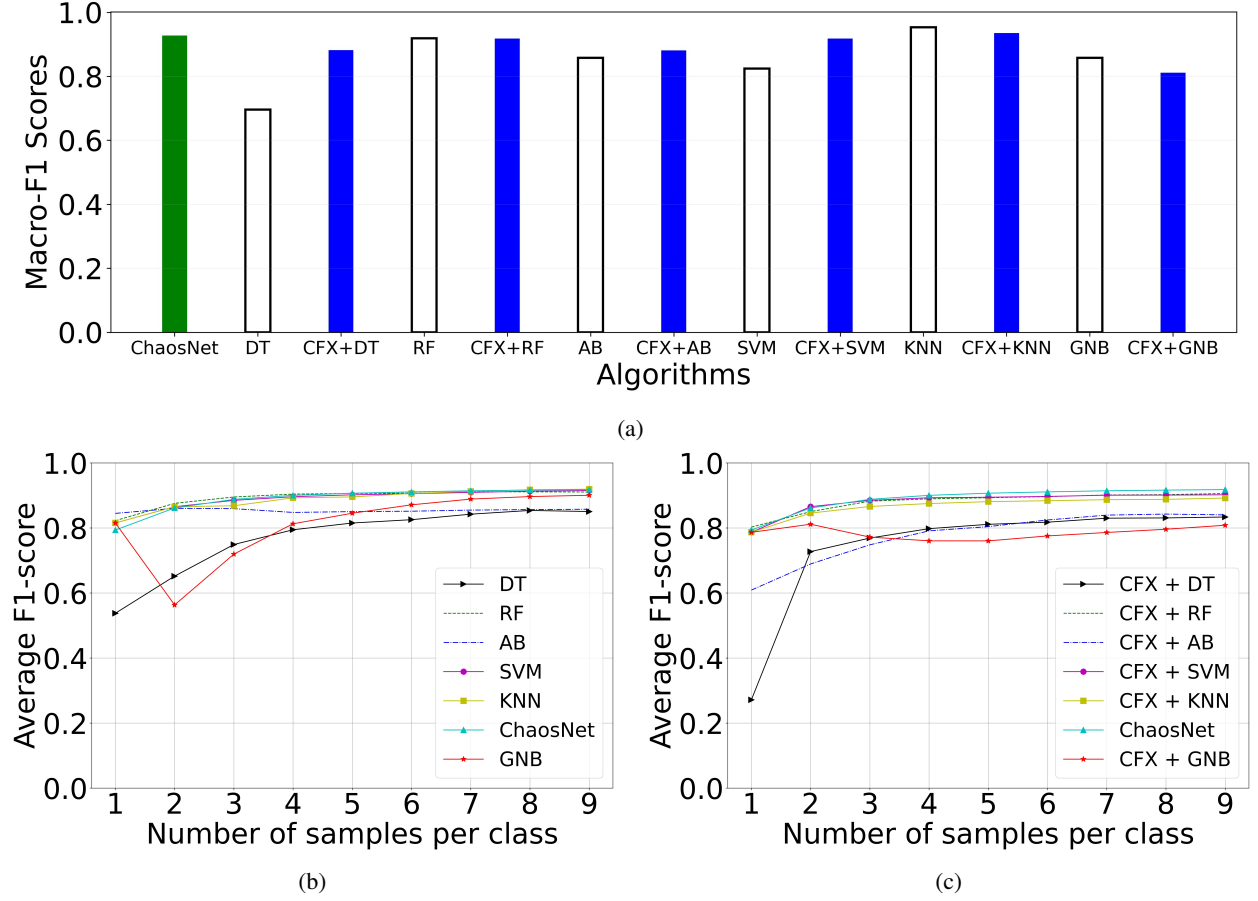


Figure 8: *Breast Cancer Wisconsin*. (a) High training sample regime. (b) Comparative performance of stand-alone algorithms in the low training sample regime. (c) Comparative performance of CFX+ML algorithms in the low training sample regime.

4.4.7 Results for Statlog (Heart)

The tuned hyperparameters used and all experiment results for the *Statlog (Heart)* dataset are available in Table 10 and Figure 9 respectively.

Table 10: Hyperparameters used for *Statlog (Heart)* dataset for high and low training sample regime experiments.

Hyperparameter	Tuned Value
q	0.080
b	0.060
ϵ	0.170

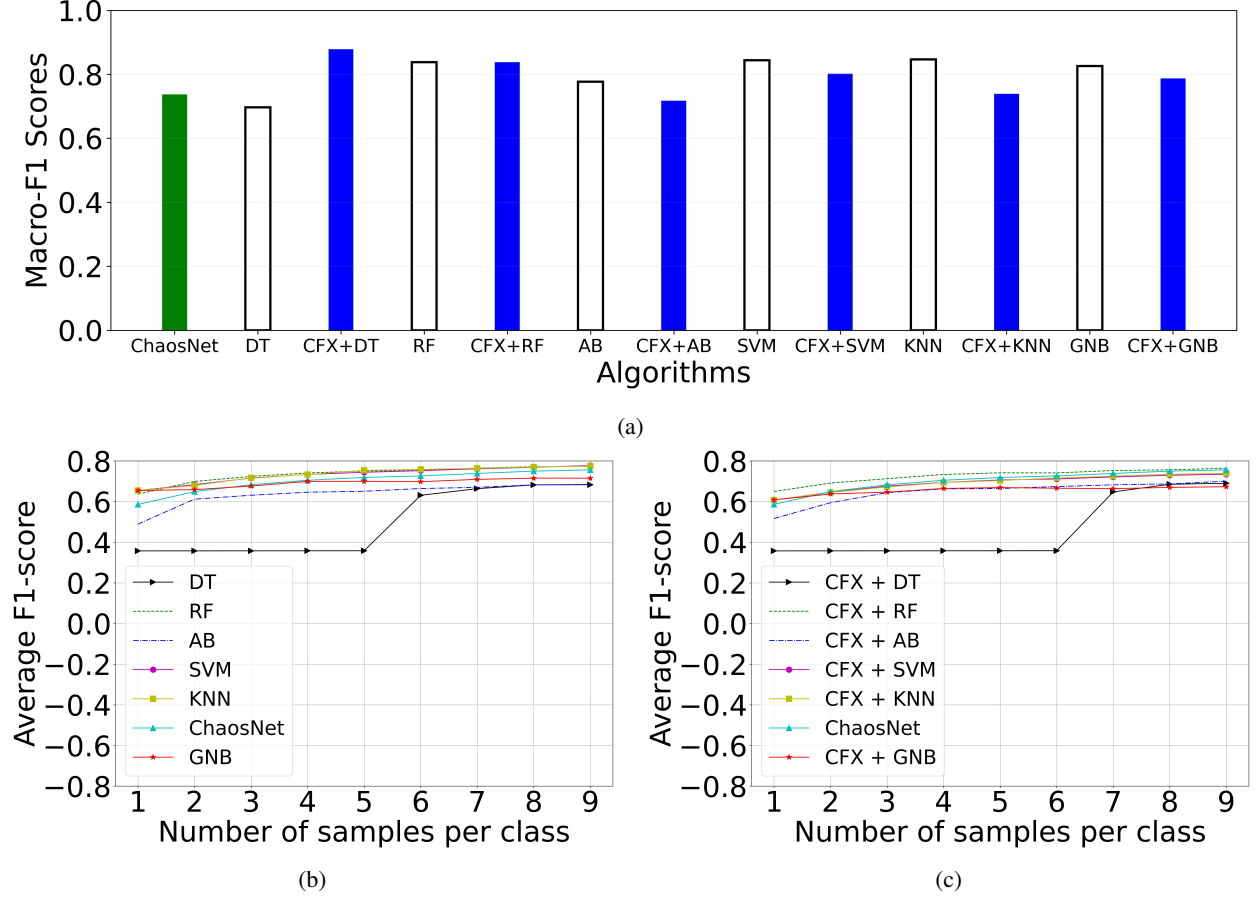


Figure 9: *Statlog (Heart)*. (a) High training sample regime. (b) Comparative performance of stand-alone algorithms in the low training sample regime. (c) Comparative performance of CFX+ML algorithms in the low training sample regime.

4.4.8 Results for Seeds

The tuned hyperparameters used and all experiment results for the *Seeds* dataset are available in Table 11 and Figure 10 respectively.

Table 11: Hyperparameters used for *Seeds* dataset for high and low training sample regime experiments.

Hyperparameter	Tuned Value
q	0.020
b	0.070
ϵ	0.238

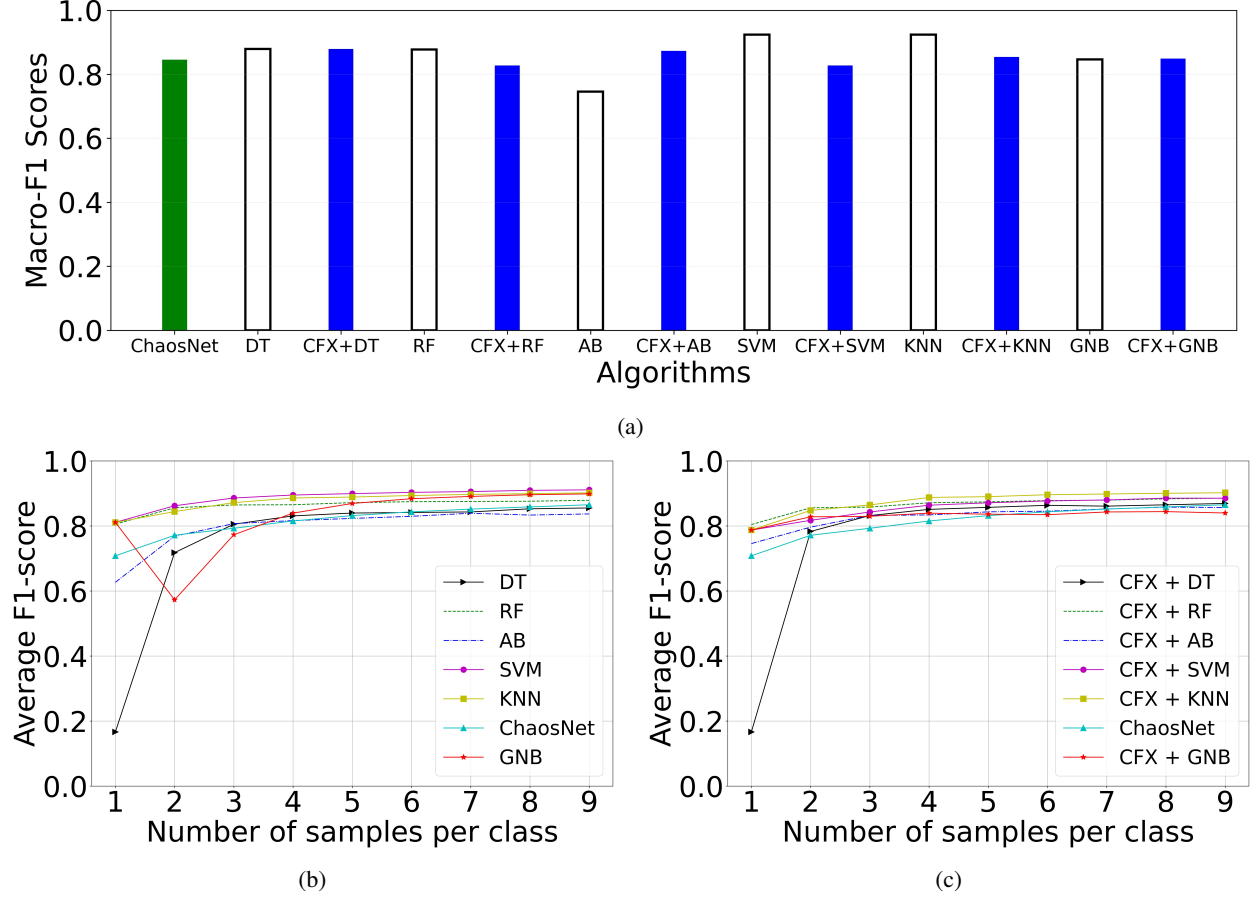


Figure 10: *Seeds*. (a) High training sample regime. (b) Comparative performance of stand-alone algorithms in the low training sample regime. (c) Comparative performance of CFX+ML algorithms in the low training sample regime.

4.4.9 Results for Free Spoken Digit Dataset (FSDD)

The tuned hyperparameters used and all experiment results for the *FSDD* dataset are available in Table 12 and Figure 11 respectively.

Table 12: Hyperparameters used for *FSDD* dataset for high and low training sample regime experiments [18]).

Hyperparameter	Tuned Value
q	0.340
b	0.499
ϵ	0.178

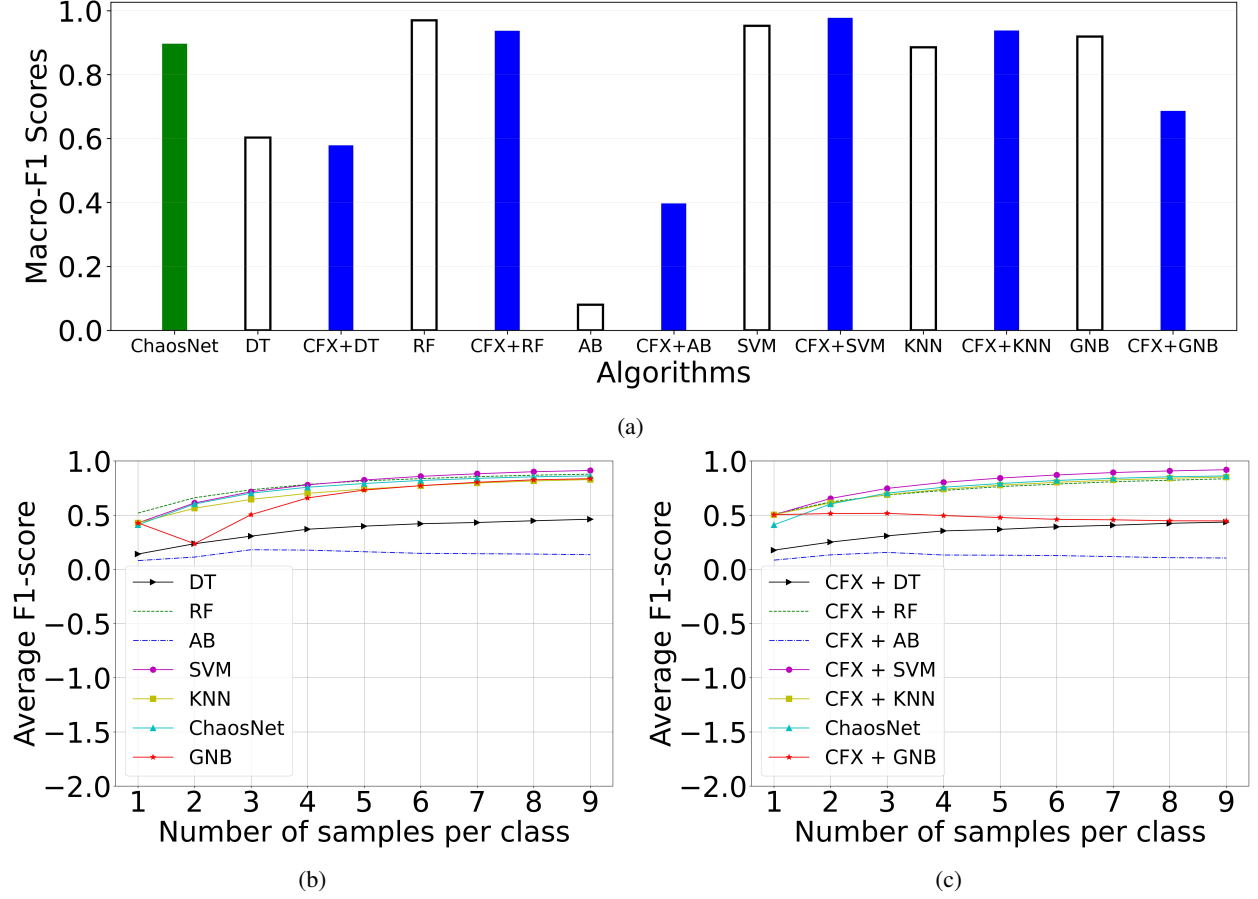


Figure 11: *Free Spoken Digit Dataset*. (a) High training sample regime. (b) Comparative performance of stand-alone algorithms in the low training sample regime. (c) Comparative performance of CFX+ML algorithms in the low training sample regime.

5 Discussion

5.1 High Training Sample Regime

The overall comparative performance of different algorithms is provided in Table 13. In the high training sample regime, the efficacy of using CFX features is evident from Table 13 for *Iris*, *Ionosphere*, *Haberman's Survival*, *Statlog (Heart)* and *FSDD*. While *Iris* is a balanced dataset, *Ionosphere*, *Haberman's Survival* and *Statlog (Heart)* are imbalanced. Through this, a versatility in the algorithm's ability to perform with both balanced and imbalanced datasets can be established.

The performance boost after using CFX features is calculated as follows:

$$Boost = \left(\frac{F1_{CFX+ML} - F1_{ML}}{F1_{ML}} \right) \cdot 100\%, \quad (11)$$

where $F1_{ML}$ and $F1_{CFX+ML}$ refers to the macro F1-score for the stand-alone ML algorithm and the hybrid NL (CFX+ML) algorithm respectively.

Table 13: Overall comparative performance of different algorithms in the high training sample regime. Percentages in parenthesis indicate the *Boost* computed using Eq 11.

Dataset	ChaosNet (Macro F1-Score)	Best Algorithm	Best Macro F1-Score
Iris	1.0	ChaosNet, RF, KNN CFX+DT (3.41 %), CFX+RF (0 %)	1.0
Ionosphere	0.860	CFX+KNN (14.37 %)	0.939
Wine	0.976	GNB	1.0
Bank Note Authentication	0.845	SVM, KNN	0.993
Haberman's Survival	0.560	CFX+AB (20.59 %)	0.609
Breast Cancer Wisconsin	0.927	<i>k</i> -NN	0.954
Statlog (Heart)	0.738	CFX+DT (25.97 %)	0.878
Seeds	0.845	KNN	0.924
FSDD	0.897	CFX+SVM (2.73 %)	0.978

5.2 Low Training Sample Regime

Table 14 demonstrates the overall performance of all datasets in the low training sample regime after employing the CFX features. A \checkmark refers to a performance boost of ML algorithms after using CFX features. CFX features have shown an evident improvement in performance for *Ionosphere*, *Haberman's Survival*, *Statlog (Heart)*, *Seeds* and *FSDD*. 150 random trials of training in the low training sample regime with 1, 2, \dots , 9 samples per class are performed. The 150 random trials of training ensures the model does not overfit.

Table 14: Overall performance boost using CFX features in the low training sample regime. A \checkmark refers to a performance boost of ML algorithms after using CFX features. We report (*Minimum*, *Maximum*) of *Boost* values only in these instances.

Dataset	DT	RF	AB	SVM	KNN	GNB
Iris						
Ionosphere	\checkmark (0.88%, 17.63%)	\checkmark (0.15%, 18.01%)	\checkmark (0.83%, 10.71%)	\checkmark (1.15%, 17.60%)	\checkmark (0.80%, 17.60%)	
Wine						
Bank Note Authentication						
Haberman's Survival	\checkmark (0.0%, 21.59%)	\checkmark (8.43%, 144.38%)		\checkmark (2.19%, 6.43%)	\checkmark (3.16%, 8.85%)	
Breast Cancer Wisconsin						
Statlog (Heart)	\checkmark (0.0%, 1.05%)		\checkmark (0.69%, 5.58%)			
Seeds	\checkmark (0.0%, 9.08%)	\checkmark (0.01%, 0.84%)	\checkmark (1.56%, 19.02%)		\checkmark (0.04%, 0.43%)	
FSDD				\checkmark (0.76%, 17.63%)	\checkmark (2.76%, 17.63%)	

5.3 Inferences based on consistency of algorithms across all datasets

The consistency of an algorithm can be inferred by evaluating the range of minimum and maximum macro F1-scores produced by it in the high training sample regime. Table 15 shows the ranges of macro F1-scores of different algorithms, measured across all nine datasets used in the research. The provided format for the range of macro F1-scores in Table 15 is [Minimum, Maximum]. ChaosNet ranks second in the least difference between the maximum and minimum macro F1-scores. This observation owes to the consistency and tolerance towards dataset diversity in ChaosNet. In algorithms such as AdaBoost (AB) and Support Vector Machine (SVM), a relatively low difference between F1-scores is realised after the usage of CFX features. Gaussian Naive Bayes (GNB) shows the least difference between F1-scores. Along datasets of different domains considered in this study, the performance of ChaosNet can be seen as comparable with GNB.

Table 15: Depiction of consistency of algorithms across all nine datasets used in this study (high training sample regime). The minimum and maximum macro F1-scores for each algorithm corresponding to all nine datasets are provided in the format: [Minimum, Maximum].

Stand-alone ML		CFX + ML	
Algorithm	F1-Score Range	Algorithm	F1-Score Range
ChaosNet	[0.56, 1.0]	-	-
DT	[0.516, 0.967]	CFX + DT	[0.482, 1.0]
RF	[0.56, 1.0]	CFX + RF	[0.398, 1.0]
AB	[0.08, 0.985]	CFX + AB	[0.397, 0.925]
SVM	[0.437, 0.993]	CFX + SVM	[0.447, 0.978]
KNN	[0.48, 1.0]	CFX + KNN	[0.455, 0.971]
GNB	[0.572, 1.0]	CFX + GNB	[0.535, 0.976]

5.4 Limitations

With the current implementation of the ChaosFEX algorithm, computation of image datasets is a costly process. This may limit the use of NL architectures in practical situations involving images.

Furthermore, NL architectures have been based on certain assumptions. One assumption revolves around the separability of data. NL assumes that applying a nonlinear chaotic transformation will result in separable data suitable for classification, which may not be true in all cases. As it stands, the input layer of NL treats input attributes as independent of each other. It establishes no connection between the neurons for each input attribute. This limitation can be addressed by using coupled chaotic neurons in the input layer. Currently, we have not considered multi-layered NL (Deep-NL) which could significantly enhance performance (by careful choice of coupling between adjacent layers). Another limitation of the NL architectures is the lack of a principled approach to tune the best hyperparameters for a classification task. Currently, cross-validation experiments are used to tune the hyperparameters. The connection between the degree of chaos as measured by lyapunov exponent [34]) and learnability is also worth exploring for future research.

6 Conclusion

Decision making under the presence of rare events is a challenging problem in the ML community. This is because rare events have limited data instances, and this problem boils down to imbalanced learning. In this work, we have evaluated the effectiveness of *ChaosFEX* (CFX) feature transformation used in *Neurochaos Learning* (NL) architectures for imbalanced learning. Nine benchmark datasets were used in this study to bring out this evaluation. Seven out of nine datasets used are imbalanced (Refer to Table 1). This paper accomplishes a comparative study on the performance of NL architecture: ChaosNet and CFX+ML with classical Machine Learning (ML) algorithms. The obtained results reflect an evident performance boost in terms of macro F1-score after a *nonlinear chaotic transformation* (ChaosFEX or CFX features). Additionally, the efficacy of CFX features can be observed in five out of nine balanced and imbalanced datasets in the high training sample regime, with a boost ranging from **2.73%** (*Free Spoken Digit Dataset*) to **25.97%** (*Statlog - Heart*). In the low training sample regime, the integration of CFX features has boosted the performance of classical ML algorithms in five datasets, from a total of nine datasets. A maximum boost of **144.38%** on the *Haberman's Survival* dataset using CFX+RF is obtained. Refer to Table 13 and 14 for the detailed performance boost using CFX features. This is the first study thoroughly evaluating the performance of NL in the imbalanced learning scenario.

NL is a unique combination of chaos and noise-enhanced classification. The enormous flexibility of NL offers endless possibilities for development of novel NL: chaos-based-hybrid ML models that suit the application at hand. As new ML algorithms get invented, they can be readily combined in the NL framework. We foresee exciting combinations of CFX with DL and other ML algorithms in the future.

7 Acknowledgments

Deeksha Sethi is thankful to Saneesh Cleatus T, Associate Professor, BMS Institute of Technology and Management for enabling her with this research opportunity. Sethi dedicates this work to her family. Harikrishnan N. B. thanks “The University of Trans-Disciplinary Health Sciences and Technology (TDU)” for permitting this research as part of the PhD programme. The authors gratefully acknowledge the financial support of Tata Trusts. The authors acknowledge the computational facility supported by NIAS Consciousness Studies Programme.

Declarations

- Funding: The authors gratefully acknowledge the financial support of Tata Trusts.
- Conflicts of Interest/Competing interests: There is no conflict of interest or competing interests.
- Ethics approval: Not Applicable.
- Consent to participate: Not Applicable.
- Consent for publication: Not Applicable.
- Availability of data and materials: Not Applicable.
- Code availability: The codes used in this research are available in the following link: <https://github.com/deeksha-sethi03/nl-imbalanced-learning>.
- Authors’ contributions:
 - Conceptualization: Harikrishnan NB
 - Methodology: Harikrishnan NB
 - Formal analysis and investigation: Deeksha Sethi, Harikrishnan NB, Nithin Nagaraj
 - Code implementation: Deeksha Sethi (Template codes provided by Harikrishnan NB)
 - Writing - original draft preparation: Deeksha Sethi, Harikrishnan NB
 - Writing - review and editing: Deeksha Sethi, Harikrishnan NB, Nithin Nagaraj
 - Funding acquisition: Nithin Nagaraj
 - Resources: Consciousness Studies Programme, National Institute of Advanced Studies
 - Supervision: Harikrishnan NB, Nithin Nagaraj

References

- [1] Joel Lehman, Jeff Clune, and Sebastian Risi. An anarchy of methods: Current trends in how intelligence is abstracted in ai. *IEEE Intelligent Systems*, 29(6):56–62, 2014.
- [2] Melanie Mitchell. *Artificial intelligence: A guide for thinking humans*. 2019.
- [3] Guo Haixiang, Li Yijing, Jennifer Shang, Gu Mingyun, Huang Yuanyue, and Gong Bing. Learning from class-imbalanced data: Review of methods and applications. *Expert Systems with Applications*, 73:220–239, 2017.
- [4] Maher Maalouf and Theodore B Trafalis. Robust weighted kernel logistic regression in imbalanced and rare events data. *Computational Statistics & Data Analysis*, 55(1):168–183, 2011.
- [5] Marco Ciotti, Massimo Ciccozzi, Alessandro Terrinoni, Wen-Can Jiang, Cheng-Bin Wang, and Sergio Bernardini. The covid-19 pandemic. *Critical reviews in clinical laboratory sciences*, 57(6):365–388, 2020.
- [6] Antoni Trilla, Guillem Trilla, and Carolyn Daer. The 1918 “Spanish Flu” in Spain. *Clinical Infectious Diseases*, 47(5):668–673, 09 2008.
- [7] Craig Beaman, Ashley Barkworth, Toluwalope David Akande, Saqib Hakak, and Muhammad Khurram Khan. Ransomware: Recent advances, analysis, challenges and future research directions. *Computers & Security*, 111:102490, 2021.

- [8] Suvasini Panigrahi, Amlan Kundu, Shamik Sural, and Arun K Majumdar. Credit card fraud detection: A fusion approach using dempster–shafer theory and bayesian learning. *Information Fusion*, 10(4):354–363, 2009.
- [9] Charles Elkan. The foundations of cost-sensitive learning. In *International joint conference on artificial intelligence*, volume 17, pages 973–978. Lawrence Erlbaum Associates Ltd, 2001.
- [10] Nitesh V Chawla, Kevin W Bowyer, Lawrence O Hall, and W Philip Kegelmeyer. Smote: synthetic minority over-sampling technique. *Journal of artificial intelligence research*, 16:321–357, 2002.
- [11] Muhammad Atif Tahir, Josef Kittler, Krystian Mikolajczyk, and Fei Yan. A multiple expert approach to the class imbalance problem using inverse random under sampling. In *International workshop on multiple classifier systems*, pages 82–91. Springer, 2009.
- [12] Ludmila I Kuncheva and William J Faithfull. Pca feature extraction for change detection in multidimensional unlabeled data. *IEEE transactions on neural networks and learning systems*, 25(1):69–80, 2013.
- [13] OO Ogundile, AM Usman, OP Babalola, and DJJ Versfeld. Dynamic mode decomposition: A feature extraction technique based hidden markov model for detection of mysticetes’ vocalisations. *Ecological Informatics*, 63:101306, 2021.
- [14] Md Afzal Hossan, Sheeraz Memon, and Mark A Gregory. A novel approach for mfcc feature extraction. In *2010 4th International Conference on Signal Processing and Communication Systems*, pages 1–5. IEEE, 2010.
- [15] Yu-Xiong Wang and Yu-Jin Zhang. Nonnegative matrix factorization: A comprehensive review. *IEEE Transactions on knowledge and data engineering*, 25(6):1336–1353, 2012.
- [16] Vaijayanthi Nagarajan, Elizabeth Caroline Britto, and Senthilvel Murugan Veeraputhiran. Feature extraction based on empirical mode decomposition for automatic mass classification of mammogram images. *Medicine in Novel Technology and Devices*, 1:100004, 2019.
- [17] Harikrishnan Nellippallil Balakrishnan, Aditi Kathpalia, Snehanishu Saha, and Nithin Nagaraj. Chaosnet: A chaos based artificial neural network architecture for classification. *Chaos: An Interdisciplinary Journal of Nonlinear Science*, 29(11):113125, 2019.
- [18] NB Harikrishnan and Nithin Nagaraj. When noise meets chaos: Stochastic resonance in neurochaos learning. *Neural Networks*, 143:425–435, 2021.
- [19] Frederico AC Azevedo, Ludmila RB Carvalho, Lea T Grinberg, José Marcelo Farfel, Renata EL Ferretti, Renata EP Leite, Wilson Jacob Filho, Roberto Lent, and Suzana Herculano-Houzel. Equal numbers of neuronal and nonneuronal cells make the human brain an isometrically scaled-up primate brain. *Journal of Comparative Neurology*, 513(5):532–541, 2009.
- [20] Henri Korn and Philippe Faure. Is there chaos in the brain? ii. experimental evidence and related models. *Comptes rendus biologiques*, 326(9):787–840, 2003.
- [21] Harikrishnan NB, Pranay SY, and Nithin Nagaraj. A neurochaos learning architecture for genome classification. *arXiv preprint arXiv:2010.10995*, 2020.
- [22] Aditi Kathpalia, Nithin Nagaraj, et al. Cause-effect preservation and classification using neurochaos learning. *arXiv preprint arXiv:2201.12181*, 2022.
- [23] NB Harikrishnan and Nithin Nagaraj. Neurochaos inspired hybrid machine learning architecture for classification. In *2020 International Conference on Signal Processing and Communications (SPCOM)*, pages 1–5. IEEE, 2020.
- [24] F. Pedregosa, G. Varoquaux, A. Gramfort, V. Michel, B. Thirion, O. Grisel, M. Blondel, P. Prettenhofer, R. Weiss, V. Dubourg, J. Vanderplas, A. Passos, D. Cournapeau, M. Brucher, M. Perrot, and E. Duchesnay. Scikit-learn: Machine learning in Python. *Journal of Machine Learning Research*, 12:2825–2830, 2011.
- [25] R. A. FISHER. The use of multiple measurements in taxonomic problems. *Annals of Eugenics*, 7(2):179–188, 1936.
- [26] Dheeru Dua and Casey Graff. UCI machine learning repository, 2017.
- [27] Vincent G Sigillito, Simon P Wing, Larrie V Hutton, and Kile B Baker. Classification of radar returns from the ionosphere using neural networks. *Johns Hopkins APL Technical Digest*, 10(3):262–266, 1989.
- [28] Michele Forina, Riccardo Leardi, Armanino C, and Sergio Lanteri. *PARVUS: An Extendable Package of Programs for Data Exploration*. 01 1998.
- [29] Eugen Gillich and Volker Lohweg. Banknote authentication. 11 2010.
- [30] Shelby J Haberman. The analysis of residuals in cross-classified tables. *Biometrics*, pages 205–220, 1973.

- [31] W Nick Street, William H Wolberg, and Olvi L Mangasarian. Nuclear feature extraction for breast tumor diagnosis. In *Biomedical image processing and biomedical visualization*, volume 1905, pages 861–870. SPIE, 1993.
- [32] Zohar Jackson, César Souza, Jason Flaks, Yuxin Pan, Hereman Nicolas, and Adhish Thite. Jakobovski/free-spoken-digit-dataset: v1.0.8, August 2018.
- [33] C. Ferri, J. Hernández-Orallo, and R. Modroi. An experimental comparison of performance measures for classification. *Pattern Recognition Letters*, 30(1):27–38, 2009.
- [34] Jonathan B Dingwell. Lyapunov exponents. *Wiley encyclopedia of biomedical engineering*, 2006.

8 Supplementary Information

This is the supplementary information pertaining to the main manuscript. It contains the following – (1) description of datasets used in our study including the coding rule for the labels of different classes, (2) hyperparameter tuning details for each dataset and for each ML algorithm (Decision Tree, Random Forest, AdaBoost, SVM, k -NN) and NL algorithm (ChaosNet) used in the study, (3) the test data macro F1-scores for each algorithm in the high training sample regime for each dataset.

8.1 Dataset Description

8.1.1 Iris

Table 16: *Iris*: Rule followed for renaming of the class labels.

Class Label	Numeric Code	Number of Total Data Instances
Iris-Setosa	0	50
Iris-Versicolour	1	50
Iris-Virginica	2	50

8.1.2 Ionosphere

Table 17: *Ionosphere*: Rule followed for renaming of the class labels.

Class Label	Numeric Code	Number of Total Data Instances
b (Bad)	0	126
g (Good)	1	225

8.1.3 Wine

Table 18: *Wine*: Rule followed for renaming of the class labels.

Class Label	Numeric Code	Number of Total Data Instances
1	0	59
2	1	71
3	2	48

8.1.4 Bank Note Authentication

Table 19: *Bank Note Authentication*: Rule followed for renaming of the class labels.

Class Label	Numeric Code	Number of Total Data Instances
0 (Genuine)	0	762
1 (Forgery)	1	610

8.1.5 Haberman's Survival

Table 20: *Haberman's Survival*: Rule followed for renaming of the class labels.

Class Label	Numeric Code	Number of Total Data Instances
1 (< 5yrs)	0	225
2 (\geq 5yrs)	1	81

8.1.6 Breast Cancer Wisconsin

Table 21: *Breast Cancer Wisconsin*: Rule followed for renaming of the class labels.

Class Label	Numeric Code	Number of Total Data Instances
M (Malignant)	0	212
B (Benign)	1	357

8.1.7 Statlog (Heart)

Table 22: *Statlog (Heart)*: Rule followed for renaming of the class labels.

Class Label	Numeric Code	Number of Total Data Instances
1 (Absence)	0	150
2 (Presence)	1	120

8.1.8 Seeds

Table 23: *Seeds*: Rule followed for renaming of the class labels.

Class Label	Numeric Code	Number of Total Data Instances
1.0 (Kama)	0	70
2.0 (Rosa)	1	70
3.0 (Canadian)	2	70

8.1.9 FSDD

Table 24: *FSDD*: Rule followed for renaming of the class labels.

Class Label	Numeric Code	Number of Total Data Instances
0	0	50
1	1	50
2	2	50
3	3	50
4	4	46
5	5	41
6	6	50
7	7	50
8	8	43
9	9	50

8.2 Hyperparameter Tuning

The hyperparameter tuning for all algorithms for the respective datasets are provided below:

8.2.1 Decision Tree

Following are the hyperparameters tuned for Decision Tree:

1. **min_samples_leaf**: Defines the minimum number of samples required for a leaf node in the decision tree. It is tuned from 1 to 10 with a step-size of 1.
2. **max_depth**: Declares the maximum depth to which a decision tree can be grown. It is tuned from 1 to 10 with a step-size of 1.
3. **ccp_alpha**: A numpy array of alpha values obtained by devising Cost Complexity Pruning on the original decision tree. This array is obtained using the *cost_complexity_pruning_path*.

All remaining hyperparameters offered by scikit-learn are retained in their default forms. The results of hyperparameter tuning for Decision Tree are available in Table 25 and 26.

Table 25: **Decision Tree**: Tuned hyperparameters for all nine datasets (Part I). The performance metric used for the provided results is macro F1-score.

Dataset	Implementation	Tuned Hyperparameters	F1 Score
Iris	Stand-Alone Decision Tree	$min_samples_leaf = 3$	0.931
		$max_depth = 3$	
		$ccp_alpha = 0.0$	
	ChaosFEX + Decision Tree	$min_samples_leaf = 3$	0.955
		$max_depth = 4$	
		$ccp_alpha = 0.0$	
		$q = 0.21$	
		$b = 0.969$	
		$\epsilon = 0.13$	
Ionosphere	Stand-Alone Decision Tree	$min_samples_leaf = 1$	0.882
		$max_depth = 2$	
		$ccp_alpha = 0.0$	
	ChaosFEX + Decision Tree	$min_samples_leaf = 1$	0.921
		$max_depth = 7$	
		$ccp_alpha = 0.0$	
		$q = 0.21$	
		$b = 0.969$	
		$\epsilon = 0.22$	
Wine	Stand-Alone Decision Tree	$min_samples_leaf = 1$	0.916
		$max_depth = 3$	
		$ccp_alpha = 0.0$	
	ChaosFEX + Decision Tree	$min_samples_leaf = 1$	0.949
		$max_depth = 6$	
		$ccp_alpha = 0.0$	
		$q = 0.21$	
		$b = 0.969$	
		$\epsilon = 0.07$	
Bank Note Authentication	Stand-Alone Decision Tree	$min_samples_leaf = 1$	0.977
		$max_depth = 8$	
		$ccp_alpha = 0.0$	
	ChaosFEX + Decision Tree	$min_samples_leaf = 1$	0.961
		$max_depth = 6$	
		$ccp_alpha = 0.000836$	
		$q = 0.080$	
		$b = 0.250$	
		$\epsilon = 0.233$	
Haberman's Survival	Stand-Alone Decision Tree	$min_samples_leaf = 4$	0.614
		$max_depth = 6$	
		$ccp_alpha = 0.005389$	
	ChaosFEX + Decision Tree	$min_samples_leaf = 2$	0.648
		$max_depth = 8$	
		$ccp_alpha = 0.005389$	
		$q = 0.81$	
		$b = 0.14$	
		$\epsilon = 0.003$	

8.2.2 Random Forest

Following are the hyperparameters tuned for Random Forest:

1. **n_estimators**: Defines the number of trees in the forest being grown. The values are tuned from the array [1, 10, 100, 1000, 10000].
2. **max_depth**: Declares the maximum depth each tree the the forest is allowed to have. It is tuned from 1 to 10 with a step-size of 1.

Table 26: **Decision Tree**: Tuned hyperparameters for all nine datasets (Part II). The performance metric used for the provided results is macro F1-score.

Dataset	Implementation	Tuned Hyperparameters	F1 Score
Breast Cancer Wisconsin (Diagnostic)	Stand-Alone Decision Tree	$min_samples_leaf = 1$	0.920
		$max_depth = 4$	
		$ccp_alpha = 0.0$	
	ChaosFEX + Decision Tree	$min_samples_leaf = 2$	0.945
		$max_depth = 8$	
		$ccp_alpha = 0.005595$	
		$q = 0.930$	
		$b = 0.490$	
		$\epsilon = 0.159$	
Statlog (Heart)	Stand-Alone Decision Tree	$min_samples_leaf = 6$	0.779
		$max_depth = 3$	
		$ccp_alpha = 0.006818$	
	ChaosFEX + Decision Tree	$min_samples_leaf = 7$	0.786
		$max_depth = 4$	
		$ccp_alpha = 0.0$	
		$q = 0.08$	
		$b = 0.06$	
		$\epsilon = 0.17$	
Seeds	Stand-Alone Decision Tree	$min_samples_leaf = 2$	0.918
		$max_depth = 4$	
		$ccp_alpha = 0.005844$	
	ChaosFEX + Decision Tree	$min_samples_leaf = 2$	0.949
		$max_depth = 5$	
		$ccp_alpha = 0.0$	
		$q = 0.02$	
		$b = 0.07$	
		$\epsilon = 0.238$	
FSDD	Stand-Alone Decision Tree	$min_samples_leaf = 1$	0.536
		$max_depth = 9$	
		$ccp_alpha = 0.0099206$	
	ChaosFEX + Decision Tree	$min_samples_leaf = 1$	0.537
		$max_depth = 10$	
		$ccp_alpha = 0.0061384$	
		$q = 0.34$	
		$b = 0.499$	
		$\epsilon = 0.178$	

All remaining hyperparameters offered by scikit-learn are retained in their default forms. The results of hyperparameter tuning for Random Forest are available in Table 27 and 28

Table 27: **Random Forest**: Tuned hyperparameters for all nine datasets (Part I). The performance metric used for the provided results is macro F1-score.

Dataset	Implementation	Tuned Hyperparameters	F1 Score
Iris	Stand-Alone Random Forest	$n_estimators = 100$	0.944
		$max_depth = 3$	
	ChaosFEX + Random Forest	$n_estimators = 10$	0.944
		$max_depth = 5$	
		$q = 0.21$	
		$b = 0.969$	
Ionosphere	Stand-Alone Random Forest	$n_estimators = 10000$	0.923
		$max_depth = 4$	
	ChaosFEX + Random Forest	$n_estimators = 100$	0.928
		$max_depth = 10$	
		$q = 0.21$	
Wine	Stand-Alone Random Forest	$n_estimators = 10$	0.980
		$max_depth = 4$	
	ChaosFEX + Random Forest	$n_estimators = 10$	0.987
		$max_depth = 5$	
		$q = 0.21$	
Bank Note Authentication	Stand-Alone Random Forest	$n_estimators = 100$	0.991
		$max_depth = 8$	
	ChaosFEX + Random Forest	$n_estimators = 100$	0.967
		$max_depth = 7$	
		$q = 0.080$	
Haberman's Survival	Stand-Alone Random Forest	$n_estimators = 1$	0.621
		$max_depth = 3$	
	ChaosFEX + Random Forest	$n_estimators = 1000$	0.651
		$max_depth = 9$	
		$q = 0.810$	
Breast Cancer Wisconsin (Diagnostic)	Stand-Alone Random Forest	$n_estimators = 1000$	0.956
		$max_depth = 9$	
	ChaosFEX + Random Forest	$n_estimators = 100$	0.955
		$max_depth = 7$	
		$q = 0.930$	
		$b = 0.490$	
		$\epsilon = 0.159$	

8.2.3 AdaBoost

Following are the hyperparameters tuned for Adaptive Boosting (AdaBoost):

1. **n_estimators**: An upper limit for the number of stumps being grown. The values are tuned from the array [1, 10, 50, 100, 500, 1000, 5000, 10000].

All remaining hyperparameters offered by scikit-learn are retained in their default forms. The results of hyperparameter tuning for AdaBoost are available in Table 29.

Table 28: **Random Forest**: Tuned hyperparameters for all nine datasets (Part II). The performance metric used for the provided results is macro F1-score.

Dataset	Implementation	Tuned Hyperparameters	F1 Score
Statlog (Heart)	Stand-Alone Random Forest	$n_estimators = 1000$	0.839
		$max_depth = 2$	
	ChaosFEX + Random Forest	$n_estimators = 10000$	0.830
		$max_depth = 4$	
		$q = 0.08$	
		$b = 0.06$	
Seeds	Stand-Alone Random Forest	$n_estimators = 100$	0.918
		$max_depth = 5$	
	ChaosFEX + Random Forest	$n_estimators = 1000$	0.941
		$max_depth = 5$	
		$q = 0.020$	
		$b = 0.070$	
FSDD	Stand-Alone Random Forest	$n_estimators = 1000$	0.9479
		$max_depth = 9$	
	ChaosFEX + Random Forest	$n_estimators = 1000$	0.921
		$max_depth = 8$	
		$q = 0.340$	
		$b = 0.499$	
		$\epsilon = 0.178$	

8.2.4 Support Vector Machine

Following are the hyperparameters tuned for Support Vector Machine (SVM):

1. **C**: Controls the bias-variance trade-off of the algorithm, known as the “*Regularization Parameter*”. It is tuned from 0.1 to 100.0 with a step-size of 0.1

All remaining hyperparameters offered by scikit-learn are retained in their default forms. The results of hyperparameter tuning for Support Vector Machine are available in Table 30.

Table 29: **AdaBoost**: Tuned hyperparameters for all nine datasets. The performance metric used for the provided results is macro F1-score.

Dataset	Implementation	Tuned Hyperparameters	F1 Score
Iris	Stand-Alone AdaBoost	$n_estimators = 50$	0.929
	ChaosFEX + AdaBoost	$n_estimators = 10$	0.915
		$q = 0.21$	
		$b = 0.969$	
Ionosphere	Stand-Alone AdaBoost	$n_estimators = 50$	0.929
	ChaosFEX + AdaBoost	$n_estimators = 500$	0.921
		$q = 0.21$	
		$b = 0.969$	
Wine	Stand-Alone AdaBoost	$n_estimators = 10$	0.896
	ChaosFEX + AdaBoost	$n_estimators = 10$	0.893
		$q = 0.21$	
		$b = 0.969$	
Bank Note Authentication	Stand-Alone AdaBoost	$n_estimators = 500$	0.999
	ChaosFEX + AdaBoost	$n_estimators = 500$	0.934
		$q = 0.080$	
		$b = 0.250$	
Haberman's Survival	Stand-Alone AdaBoost	$n_estimators = 10$	0.620
	ChaosFEX + AdaBoost	$n_estimators = 1$	0.639
		$q = 0.81$	
		$b = 0.14$	
Breast Cancer Wisconsin (Heart)	Stand-Alone AdaBoost	$n_estimators = 1000$	0.962
	ChaosFEX + AdaBoost	$n_estimators = 100$	0.952
		$q = 0.930$	
		$b = 0.490$	
Statlog (Heart)	Stand-Alone AdaBoost	$n_estimators = 10$	0.816
	ChaosFEX + AdaBoost	$n_estimators = 50$	0.815
		$q = 0.08$	
		$b = 0.06$	
Seeds	Stand-Alone AdaBoost	$n_estimators = 500$	0.563
	ChaosFEX + AdaBoost	$n_estimators = 10$	0.918
		$q = 0.020$	
		$b = 0.070$	
FSDD	Stand-Alone AdaBoost	$n_estimators = 50$	0.086
	ChaosFEX + AdaBoost	$n_estimators = 50$	0.170
		$q = 0.340$	
		$b = 0.499$	

8.2.5 k-Nearest Neighbors

Following are the hyperparameters tuned for k -Nearest Neighbors:

1. k : Defines the number of nearest training data samples to the testing data sample to be chosen. It is tuned from 1 to 6 with a step-size of 2.

Table 30: **Support Vector Machine (SVM)**: Tuned hyperparameters for all nine datasets. Only FSDD uses the ‘linear’ kernel. All remaining datasets, use the ‘rbf’ kernel. The performance metric used for the provided results is macro F1-score.

Dataset	Implementation	Tuned Hyperparameters	F1 Score
Iris	Stand-Alone SVM	$C = 4.4$	0.954
	ChaosFEX + SVM	$C = 38.7$	0.958
		$q = 0.21$	
		$b = 0.969$	
Ionosphere	Stand-Alone SVM	$C = 2.6$	0.934
	ChaosFEX + SVM	$C = 3.4$	0.926
		$q = 0.21$	
		$b = 0.969$	
Wine	Stand-Alone SVM	$C = 0.6$	0.975
	ChaosFEX + SVM	$C = 16.0$	0.958
		$q = 0.21$	
		$b = 0.969$	
Bank Note Authentication	Stand-Alone SVM	$C = 1.3$	1.0
	ChaosFEX + SVM	$C = 16.8$	0.965
		$q = 0.080$	
		$b = 0.250$	
Haberman’s Survival	Stand-Alone SVM	$C = 19.8$	0.597
	ChaosFEX + SVM	$C = 15.7$	0.609
		$q = 0.81$	
		$b = 0.14$	
Breast Cancer Wisconsin (Diagnostic)	Stand-Alone SVM	$C = 16.0$	0.981
	ChaosFEX + SVM	$C = 20.3$	0.948
		$q = 0.930$	
		$b = 0.490$	
Statlog (Heart)	Stand-Alone SVM	$C = 0.2$	0.852
	ChaosFEX + SVM	$C = 2.5$	0.825
		$q = 0.08$	
		$b = 0.06$	
Seeds	Stand-Alone SVM	$C = 0.9$	0.948
	ChaosFEX + SVM	$C = 2.4$	0.909
		$q = 0.020$	
		$b = 0.070$	
FSDD	Stand-Alone SVM (linear kernel)	$C = 0.7$	0.952
	ChaosFEX + SVM (linear kernel)	$C = 6.1$	0.978
		$q = 0.340$	
		$b = 0.499$	
		$\epsilon = 0.178$	

All remaining hyperparameters offered by scikit-learn are retained in their default forms. The results of hyperparameter tuning for k -Nearest Neighbors are available in Table 31.

Table 31: *k-Nearest Neighbors (k-NN)*: Tuned hyperparameters for all nine datasets. The performance metric used for the provided results is macro F1-score.

Dataset	Implementation	Tuned Hyperparameters	F1 Score
Iris	Stand-Alone k -NN	$k = 5$	0.944
	ChaosFEX + k -NN	$k = 1$	0.936
		$q = 0.21$	
		$b = 0.969$	
Ionosphere	Stand-Alone k -NN	$k = 1$	0.814
	ChaosFEX + k -NN	$k = 1$	0.886
		$q = 0.21$	
		$b = 0.969$	
Wine	Stand-Alone k -NN	$k = 5$	0.957
	ChaosFEX + k -NN	$k = 1$	0.966
		$q = 0.21$	
		$b = 0.969$	
Bank Note Authentication	Stand-Alone k -NN	$k = 5$	0.998
	ChaosFEX + k -NN	$k = 3$	0.967
		$q = 0.080$	
		$b = 0.250$	
Haberman's Survival	Stand-Alone k -NN	$k = 1$	0.562
	ChaosFEX + k -NN	$k = 5$	0.659
		$q = 0.81$	
		$b = 0.14$	
Breast Cancer Wisconsin (Diagnostic)	Stand-Alone k -NN	$k = 5$	0.964
	ChaosFEX + k -NN	$k = 1$	0.932
		$q = 0.930$	
		$b = 0.490$	
Statlog (Heart)	Stand-Alone k -NN	$k = 5$	0.803
	ChaosFEX + k -NN	$k = 5$	0.791
		$q = 0.08$	
		$b = 0.06$	
Seeds	Stand-Alone k -NN	$k = 5$	0.930
	ChaosFEX + k -NN	$k = 1$	0.876
		$q = 0.020$	
		$b = 0.070$	
FSDD	Stand-Alone k -NN	$k = 1$	0.834
	ChaosFEX + k -NN	$k = 1$	0.909
		$q = 0.340$	
		$b = 0.499$	

8.2.6 ChaosNet

1. q : Initial Neural Activity, it is varied from 0.01 to 0.49 with a step-size of 0.01.
2. b : Discrimination Threshold, it is varied from 0.01 to 0.49 with a step-size of 0.01.
3. ϵ : Noise Intensity, it is varied from 0.001 to 0.499 with a step-size of 0.001.

8.3 Results

8.3.1 Decision Tree

The results of all experiments using Decision Tree in the high training sample regime are shown in Table 32.

Table 32: **Decision Tree**: Experiment results (test data macro F1-scores) for all nine datasets in the high training sample regime.

Dataset	Implementation	F1 Score (Test Data)
Iris	Stand-Alone Decision Tree	0.967
	ChaosFEX + Decision Tree	1.0
Ionosphere	Stand-Alone Decision Tree	0.881
	ChaosFEX + Decision Tree	0.891
Wine	Stand-Alone Decision Tree	0.904
	ChaosFEX + Decision Tree	0.822
Bank Note Authentication	Stand-Alone Decision Tree	0.933
	ChaosFEX + Decision Tree	0.978
Haberman's Survival	Stand-Alone Decision Tree	0.516
	ChaosFEX + Decision Tree	0.482
Breast Cancer Wisconsin (Diagnostic)	Stand-Alone Decision Tree	0.696
	ChaosFEX + Decision Tree	0.882
Statlog (Heart)	Stand-Alone Decision Tree	0.697
	ChaosFEX + Decision Tree	0.878
Seeds	Stand-Alone Decision Tree	0.880
	ChaosFEX + Decision Tree	0.880
FSDD	Stand-Alone Decision Tree	0.603
	ChaosFEX + Decision Tree	0.579

8.3.2 Random Forest

The results of all experiments using Random Forest in the high training sample regime are shown in Table 33.

Table 33: **Random Forest**: Experiment results (test data macro F1-scores) for all nine datasets in the high training sample regime.

Dataset	Implementation	F1 Score (Test Data)
Iris	Stand-Alone Random Forest	1.0
	ChaosFEX + Random Forest	1.0
Ionosphere	Stand-Alone Random Forest	0.909
	ChaosFEX + Random Forest	0.924
Wine	Stand-Alone Random Forest	0.966
	ChaosFEX + Random Forest	0.943
Bank Note Authentication	Stand-Alone Random Forest	0.974
	ChaosFEX + Random Forest	0.978
Haberman's Survival	Stand-Alone Random Forest	0.560
	ChaosFEX + Random Forest	0.398
Breast Cancer Wisconsin (Diagnostic)	Stand-Alone Random Forest	0.919
	ChaosFEX + Random Forest	0.918
Statlog (Heart)	Stand-Alone Random Forest	0.838
	ChaosFEX + Random Forest	0.838
Seeds	Stand-Alone Random Forest	0.877
	ChaosFEX + Random Forest	0.828
FSDD	Stand-Alone Random Forest	0.970
	ChaosFEX + Random Forest	0.937

8.3.3 Adaptive Boosting (AdaBoost)

The results of all experiments using AdaBoost in the high training sample regime are shown in Table 34.

Table 34: *AdaBoost*: Experiment results (test data macro F1-scores) for all nine datasets in the high training sample regime.

Dataset	Implementation	F1 Score (Test Data)
Iris	Stand-Alone AdaBoost	0.967
	ChaosFEX + AdaBoost	0.865
Ionosphere	Stand-Alone AdaBoost	0.926
	ChaosFEX + AdaBoost	0.925
Wine	Stand-Alone AdaBoost	0.833
	ChaosFEX + AdaBoost	0.846
Bank Note Authentication	Stand-Alone AdaBoost	0.985
	ChaosFEX + AdaBoost	0.910
Haberman's Survival	Stand-Alone AdaBoost	0.505
	ChaosFEX + AdaBoost	0.609
Breast Cancer Wisconsin (Diagnostic)	Stand-Alone AdaBoost	0.858
	ChaosFEX + AdaBoost	0.881
Statlog (Heart)	Stand-Alone AdaBoost	0.777
	ChaosFEX + AdaBoost	0.717
Seeds	Stand-Alone AdaBoost	0.746
	ChaosFEX + AdaBoost	0.873
FSDD	Stand-Alone AdaBoost	0.080
	ChaosFEX + AdaBoost	0.397

8.3.4 Support Vector Machine (SVM)

The results of all experiments using Support Vector Machine (SVM) in the high training sample regime are shown in Table 35.

Table 35: *Support Vector Machine (SVM)*: Experiment results (test data macro F1-scores) for all nine datasets in the high training sample regime.

Dataset	Implementation	F1 Score (Test Data)
Iris	Stand-Alone SVM	0.966
	ChaosFEX + SVM	0.933
Ionosphere	Stand-Alone SVM	0.924
	ChaosFEX + SVM	0.909
Wine	Stand-Alone SVM	0.928
	ChaosFEX + SVM	0.896
Bank Note Authentication	Stand-Alone SVM	0.993
	ChaosFEX + SVM	0.978
Haberman's Survival	Stand-Alone SVM	0.437
	ChaosFEX + SVM	0.447
Breast Cancer Wisconsin (Diagnostic)	Stand-Alone SVM	0.824
	ChaosFEX + SVM	0.918
Statlog (Heart)	Stand-Alone SVM	0.844
	ChaosFEX + SVM	0.801
Seeds	Stand-Alone SVM	0.924
	ChaosFEX + SVM	0.827
FSDD	Stand-Alone SVM	0.952
	ChaosFEX + SVM	0.978

8.3.5 k-Nearest Neighbors

The results of all experiments using k - Nearest Neighbors in the high training sample regime are shown in Table 36.

Table 36: *k-Nearest Neighbors* (k -NN): Experiment results (test data macro F1-scores) for all nine datasets in the high training sample regime.

Dataset	Implementation	F1 Score (Test Data)
Iris	Stand-Alone k -NN	1.0
	ChaosFEX + k -NN	0.902
Ionosphere	Stand-Alone k -NN	0.821
	ChaosFEX + k -NN	0.939
Wine	Stand-Alone k -NN	0.943
	ChaosFEX + k -NN	0.873
Bank Note Authentication	Stand-Alone k -NN	0.993
	ChaosFEX + k -NN	0.971
Haberman's Survival	Stand-Alone k -NN	0.480
	ChaosFEX + k -NN	0.455
Breast Cancer Wisconsin (Diagnostic)	Stand-Alone k -NN	0.954
	ChaosFEX + k -NN	0.935
Statlog (Heart)	Stand-Alone k -NN	0.847
	ChaosFEX + k -NN	0.739
Seeds	Stand-Alone k -NN	0.924
	ChaosFEX + k -NN	0.854
FSDD	Stand-Alone k -NN	0.885
	ChaosFEX + k -NN	0.938

8.3.6 Gaussian Naive Bayes

The results of all experiments using Gaussian Naive Bayes (GNB) in the high training sample regime are shown in Table 37.

Table 37: *Gaussian Naive Bayes (GNB)*: Experiment results (test data macro F1-scores) for all nine datasets in the high training sample regime.

Dataset	Implementation	F1 Score (Test Data)
Iris	Stand-Alone GNB	0.966
	ChaosFEX + GNB	0.933
Ionosphere	Stand-Alone GNB	0.862
	ChaosFEX + GNB	0.771
Wine	Stand-Alone GNB	1.0
	ChaosFEX + GNB	0.976
Bank Note Authentication	Stand-Alone GNB	0.785
	ChaosFEX + GNB	0.781
Haberman's Survival	Stand-Alone GNB	0.572
	ChaosFEX + GNB	0.535
Breast Cancer Wisconsin (Diagnostic)	Stand-Alone GNB	0.858
	ChaosFEX + GNB	0.812
Statlog (Heart)	Stand-Alone GNB	0.826
	ChaosFEX + GNB	0.788
Seeds	Stand-Alone GNB	0.846
	ChaosFEX + GNB	0.849
FSDD	Stand-Alone GNB	0.919
	ChaosFEX + GNB	0.687